PHARMACOLOGICAL EVALUATION OF
IDAZOXAN-INDUCED NORADRENERGIC
MODULATION OF EXCITATORY AND INHIBITORY
PROCESSES IN THE DENTATE GYRUS OF THE
ANAESTHETIZED RAT

JOHN CHRISTOPHER KNIGHT

Canada

PHARMACOLOGICAL EVALUATION OF IDAZOXAN-INDUCED

NORADRENERGIC MODULATION OF EXCITATORY AND INHIBITORY

PROCESSES IN THE DENTATE GYRUS OF THE ANAESTHETIZED RAT

by

John Christopher Knight, B.Sc. (Hons.)

A thesis submitted to the School of Graduate Studies

in partial fulfilment of the requirements for the degree of

Master of Science

Division of Basic Medical Sciences

Faculty of Medicine

Memorial University of Newfoundland

January 2002

St. John's   Newfoundland

ABSTRACT

Exogenous norepinephrine (NE) potentiates the evoked potential (EP) recorded from the dentate gyrus (DG) of the hippocampus *in vivo* (Neuman and Harley, 1983; Winson and Dahl, 1985) and *in vitro* (Lacaille and Harley, 1985; Stanton and Sarvey, 1985b). Endogenous NE released by activation of the locus coeruleus (LC) system by glutamatergic (Harley and Milway, 1986; Harley and Evans, 1988) or electrical stimulation (Dahl and Winson, 1985; Assaf et al., 1979; Washburn and Moises, 1989) of the LC or its input, the nucleus paragigantocellularis (Babstock and Harley, 1992) has similar effects. Evidence suggests that the initiation of these potentiations are mediated by β-adrenergic activation and that local β-receptors in the DG play an important role in this phenomenon (Lacaille and Harley, 1985; Stanton and Sarvey, 1985b; Babstock and Harley, 1992; Washburn and Moises, 1989; Harley and Milway, 1986). NE has also been shown to excite and inhibit interneurons recorded in the DG (Rose and Pang, 1989; Clarke 1995).

Yet another method of releasing endogenous LC-NE and subsequent potentiation of the DG EP is via systemic application of the α2-antagonist idazoxan (IDA) (Cedarbaum and Aghajanian, 1978; Richter-Levin, 1991; Sara and Bergis, 1991). IDA has also been shown to result in an increase in paired-pulse inhibition in the DG (Sara and Bergis, 1991).

The present study utilized the paired-pulse paradigm and double pipette technique to examine the role of β-receptor activation in IDA-induced NE modulation of excitation and inhibition in the local circuitry of the DG. Saline and timolol-filled micropipettes were placed in the DG of urethane-anaesthetized rats. The perforant path was stimulated with

ii

paired pulses spaced at short intervals and rats were given systemic injection of IDA after baseline recroding. Evidence was demonstrated for five distinct effects of NE in the local circuitry of the DG. These were: 1) enhancement of tonic activity of somatic inhibitory interneurons at baseline via low threshold β-receptor activation; 2) increased cell firing to a constant input supported by a high-threshold direct β-receptor action on granule cell membranes; 3) a decrease in EPSP size probably due to increased feed-forward dendritic inhibition; 4) inhibition of somatic feedback disinhibition circuits (rather than an increase in inhibition per se); and 5) enhancement of firing of feedback dendritic inhibitory interneurons possibly via $\alpha 1$-receptor activation. Effects observed in the DG with IDA in the present study were compared to those observed during learning and exploration of a new environment in other studies.

ACKNOWLEDGMENTS

CONTENTS

LIST OF FIGURES

1.1 The Hippocampus and learning and memory

It has been the dream of many neurobiologists to discover the physiological basis of cognitive phenomena like learning and memory. Central to learning and memory is the part of the brain known as the hippocampus. It first became known that the hippocampus was involved in memory from studies of patients with amnesia resulting from surgical or pathological alterations to the brain. Perhaps the most famous of these is H.M. who underwent bilateral resection of the medial temporal lobe, including the hippocampus as a treatment for epilepsy. H.M. was able to remember much from before surgery but could not learn new facts or come to recognize faces of new people (Scolville and Milner, 1957). This is called anterograde amnesia. He retained working memory and the ability to form procedural memories but could no longer form declarative memories. Another patient, R. B., who was found to have ischemia-induced bilateral damage localized mainly to the CA1 region of the hippocampus, exhibited similar although less severe symptoms. This led scientists to conclude that the hippocampus was involved in consolidation of declarative memory but not working or procedural memory or memory storage. Individuals with Korakoff's syndrome, involving extensive damage to the diencephalon - a target of hippocampal efferents, show similar memory impairments.

In animals, hippocampal damage is generally associated with deficits in spatial memory; i.e. an animal's ability to navigate through its environment. One area of animal research involving the hippocampus and memory has focused on lesion studies. Lesion

1

studies involve surgically, electrically or chemically-induced damage to, destruction of, or removal of the hippocampus or its afferents or efferents and training the lesioned animal in a task which tests its ability to form and retain long-term memories of its spatial environment.

For example, initial aquisition of the Morris Water Maze task - in which animals are trained to find a platform submerged just beneath the surface in a pool of water made opaque by powdered milk - has been found to be sensitive to hippocampal lesions (Morris et al., 1982; Sutherland et al., 1982), and selective lesions of the dentate gyrus (Sutherland et al., 1983). Initial acquisition is also disrupted by lesions downstream of the hippocampus, in the subicular complex (Morris et al., 1990) and medial frontal cortical region (Sutherland et al., 1982). Lesions upstream of the hippocampus such as the perforant path, the main entorhinal input to the hippocampus (Skelton and McNamara, 1992) and lesions to the medial septum, another major input to the hippocampus (Hagan et al., 1988) also disrupt acquisition.

Hippocampal lesions have also been shown to result in deficits in delayed-non-matching-to-sample tasks (Mishkin, 1978; Zola Morgan et al., 1982; Squire, 1985) and the radial arm maze tasks (Olton, 1983; Olton, Becker and Handelmann, 1979; Olton and Papas, 1979).

A second area of animal research relating the hippocampus to learning and memory involves electrophysiology or recording of responses from the brain with electrodes. For example, O'Keefe and Dostrovsky, 1971 discovered that hippocampal neurons fire

2

selectively when an animal is in different regions or 'place fields' of an environment. A given neuron fires when the animal is in a certain area of its environment. This area is known as the cell's 'place field' and these neurons are known as 'place cells'. This discovery lead to the development of a comprehensive theory by O'Keefe and Nadel, 1978 entitled, 'The Hippocampus as a Cognitive Map.' Further understanding of hippocampal electrophysiological research necessitates knowledge of hippocampal anatomy and physiology.

1.2 The Hippocampal Formation

The hippocampus is part of the limbic system located in the medial temporal lobe, whose structures have been shown to be involved in emotion (Kluver and Bucy, 1937; Mishkin and Apenzeller, 1987), motivation (Pinel, 1993) and learning and memory (Barnes, 1988; Squire and Zola-Morgan, 1988). The limbic system is, in turn, part of the paleocortex or 'older' cortex in an evolutionary sense (Pinel, 1993). This is in contrast to the neocortex or 'newer' cortex. The name hippocampus literally means horse field referring to the shape of stained cell fields that form the shape of a seahorse. Along its long axis the hippocampus forms a sea horse or cashew shape extending from the septal nuclei rostrodorsally, behind the diencephalon, to the incipient temporal lobe caudoventrally (Amaral and Witter, 1989). The two extremes are therefore called the septal and temporal poles. The hippocampus consists of 4 cytoarchitectonically distinct

3

regions, including: 1) the dentate gyrus; 2) hippocampus proper (Ammon's Horn), subdivided into three fields (CA1, CA2 and CA3); 3) the subicular complex and 4) the entorhinal cortex. If one examines a hippocampal section in the transverse plane one can see the basic intrinsic circuitry of the hippocampus (Figure 1). Sensory information is thought to enter the hippocampus through its major input, the perforant path (PP), in the angular bundle, from entorhinal cortex to the dentate gyrus (DG). The main cell type in the DG, the granule cells, send axons called the mossy fibers to synapse with the pyramidal cells of CA3 which, in turn relay multisensory information to the pyramidal cells of CA1 via the Shaeffer collaterals. These pathways are largely unidirectional and together are termed the trisynaptic circuit. The amnesic patient, R.B. described above, proved to have a lesion which was spatially limited to pyramidal neurons in the CA1 field. Such a lesion would open the trisynaptic circuit (Squire and Zola-Morgan, 1988). According to McNaughton and Morris (1987) some computation must occur in this circuitry if learning is to be accomplished in a normal way. In rats it has been found that the dentate gyrus must be intact in order for spatial learning to occur (Sutherland et al., 1983; Walsh et al., 1986; McNaughton et al., 1989; Armstrong et al., 1993; Conrad and Roy, 1993).

CA1, in turn, sends axons to the subiculum which is responsible for the major output of the hippocampus. The subiculum sends axons to the mammillary bodies and hypothalamus via the fornix as well as axons back to entorhinal cortex which relays information back to sensory cortices. Thus there is a continuous loop from sensory cortices, through the hippocampus and back again to sensory cortices. It is thought that
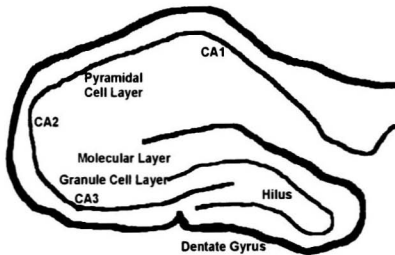
memory is born somewhere within.

Figure 1

Tranverse section through rat hippocampus illustrating cell layers

1.3 Anatomy of the Dentate Gyrus

The principal cells of the DG are the granule cells. The dentate gyrus consists of three layers: the molecular layer, the cell layer and the polymorph region or hilus (Amaral and Witter, 1989). The most obvious in a transverse section is the cell layer which consists of tightly-packed cell bodies which form a U-shape or V-shape depending on antero-posterior extent, the apex of which points medially (Figure 1). The arms of the U are termed the dorsal and ventral blades of the DG. The molecular layer, which is on the outer periphery of the U-shaped cell layer, consists of dendritic trees with which the PP and other terminals synapse. Between the blades is the polymorph layer or hilus. The granule cells send axons, the mossy fibers, into the hilus where they collateralize and then form synapses with the pyramidal cells of the CA3 region (Amaral and Witter, 1989). Found in the granule cell layer and subgranular region, but in greatest numbers in the hilus, are interneurons (Amaral, 1978). These cells form a local network in the DG and function as modulatory cells (Leranth et al., 1990). Interneurons of the DG may exert inhibitory influence upon their target cells (the granule cells) or they may inhibit other interneurons resulting in net excitatory influence on the target cells (Buckmaster and Soltesz, 1996). The interneurons are a heterogeneous group of cells whose subtypes differ in neurotransmitter, electrophysiological properties, morphological characteristics and the target of their projections (Buckmaster and Soltesz, 1996; Scharfman et al., 1990). Perhaps the main reason why interneurons were thought to exert inhibitory

6

1996). Esclapez and Houser (1995) have provided evidence that a subpopulation of GABA-containing hilar interneurons also release the peptide neurotransmitter somatostatin (SS). Sloviter and Nilaver (1987) found no co-localization of SS and GABA in hilar interneurons, thus supporting the existence of two separate populations of interneurons in the hilus.

Interneurons inhibit the principal cells by two mechanisms. In feed-back inhibition, when excitatory activity occurs in the granule cells, this activity is fed back to the interneurons by collaterals. The interneurons then exert an inhibitory influence on subsequent excitation of the granule cells (Buzaki, 1984, Sloviter, 1987). Feed-forward inhibition involves the direct excitation of interneurons by perforant path input. Interneurons then inhibit firing of target cells (Buzaki, 1984).

Another type of neuron, which appears to be glutamatergic (Amaral and Witter, 1989) and is numerous in the hilus (Amaral, 1978) is the mossy cell. Mossy cells receive input from mossy fibers and send their axons to synapse with other hilar local circuit neurons (Ribak et al., 1985; Scharfman et al., 1990) as well as others in the inner molecular zone. (Amaral and Witter, 1989). The circuitry and neurotransmitter of mossy cells implies a role in feed-back or feed-forward excitation of granule cells (Carre, 1993).

1.4 The search for the physical memory trace

How does the brain store a memory? Presumably, when we learn a new skill or form a new memory, something in the brain changes in order to encode the memory. A popular

approach used in trying to determine the neurophysiological correlate(s) of memory is to search for plasticity exhibited by brain areas involved in memory. Neuronal plasticity can be defined as the capacity of neurons to change functionally or even structurally in a relatively short period of time. Where should we look for such plasticity? What better place to start than the hippocampus? Groups of neurons in the hippocampus show plasticity of synaptic strength. Synaptic strength or efficacy refers to the effectiveness of presynaptic cell activity in inducing post-synaptic cell firing.

1.5 The measurement of synaptic efficacy - recording of the evoked field potential

The regular and parallel arrangement of hippocampal neurons is very fortunate for the electrophysiologist as it is possible to generate very large extracellular responses via stimulation of excitatory afferents (Barnes, 1988). Because the granule cell neurons are so tightly packed it is relatively easy to record extracellularly, the activity of a group of principal cells (for our purposes the granule cells of the DG) in an area called a field. It is much less difficult than recording the activity of single cells and gives a picture of how cells are responding as a group. For example, by placing a stimulating electrode in the PP one can produce a response in the DG in the millivolt (mV) range. The response can be recorded with an extracellular electrode and is a measure of excitability of a population of granule cells in the area of the recording electrode. (Andersen et al., 1966) which is referred to as the field of the electrode. This type of recording is therefore called field recording. The response can

8

be measured over time before and after some experimental manipulation. The elicited response is referred to as an evoked field potential or simply an evoked potential (EP) and, in the DG, consists of two main components, the population excitatory-post-synaptic-potential (or simply EPSP) and the population spike.

The EPSP is a measure of synaptic efficacy; a measure of current flow into the dendrites of the post-synaptic cells in the general area or field of the recording electrode. Included in its makeup are factors such as the number of perforant path fibres activated by stimulation, amount of neurotransmitter released and the sensitivity and number of postsynaptic receptors (Lomo, 1971). If measured in the molecular layer (dendrites) the EPSP is a negative-going wave reflecting an inward current flow. After the recording electrode passes into the granule cell layer (cell bodies) the evoked potential reverses and appears as a positive-going wave reflecting outward current flow.

If the total sum of EPSPs becomes great enough, granule cell action potentials occur. The second component of the evoked potential, the population spike, is actually a measure of postsynaptic cell firing. At the cell layer, it appears as a negative deflection superimposed onto the positive-going EPSP. The population spike amplitude (PSA) reflects the synchrony of granule cell firing and the number of granule cells generating action potentials (Andersen et al., 1971; Bliss and Lomo, 1973 and Lomo 1971). In the present study the measures of the evoked potential used are EPSP Slope (Figure 2A), PSA (Figure 2B) and population spike latency (PSL) (measured from stimulus artifact to peak of population spike - Figure 2C).
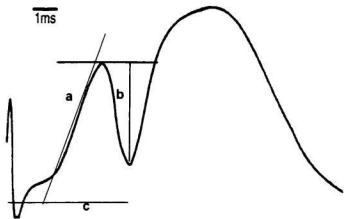
Figure 2

Perforant-path evoked potential recorded from cell layer of the dentate gyrus illustrating measured parameters

As discovered in rabbit hippocampus by Bliss and Lomo (1973) application of a high-frequency stimulus train or tetanus to the PP results in a long-lasting enhancement of the dentate gyrus EP. This widely-studied form of synaptic plasticity is called long-term potentiation (LTP) and is considered a prime candidate for a mechanism of memory storage in the mammalian brain (Teyler and Discenna, 1984). Initiation of LTP in the DG has been attributed to glutamate receptors of the NMDA (N-methyl-D-asparate) receptor subtype. As an illustration, Butcher et al. (1990) found that the NMDA receptor antagonist D-2-amino-5-phosphonovalerate caused a dose-related impairment of both LTP and spatial learning. NMDA receptors are glutamate-dependent and, also, voltage-dependent due to blockade by magnesium ions. Temporal summation of EPSPs by a tetanus brings the membrane potential to a level where magnesium ions no longer block the channels, thereby allowing their activation.

Neuronal excitability and transmission through the hippocampal formation have been found to be modulated by sensory input and by behavioral state. For example, Herreras et al. (1988) found that DG responses to PP stimulation were enhanced during periods of sensory stimulation (produced by gentle stroking of the animal's fur) and the cellular excitability increased as judged by the shift to the left of the EPSP-PSA relation. Opposite effects were seen in CA1. The results demonstrate that sensory stimulation causes modulation of information transfer through the hippocampus. The modification of

11

hippocampal transmission may serve to gate the information reaching CA1 and the DG.

Winson and Abzug (1978) found that the monosynaptic PSA recorded in the upper blade of the dentate gyrus (DG) was greater in slow-wave sleep (SWS) than during alertness and was intermediate in the awake state and REM sleep. The monosynaptic EPSP recorded in the DG, in contrast to the PSA, was greater in magnitude during alertness than during SWS. The primary afferent volley was also recorded at high gain in the DG. The amplitude of this was found to be dependent solely on stimulus intensity and not on behavioral state. Thus the number of neurons responding while the animal was alert was small while the number was much greater during SWS and REM sleep. These findings are interpreted in terms of the existence of a behaviorally-dependent gate of neural transmission in the hippocampus. The granule cell membranes in the DG are relatively hyperpolarized during alertness compared with SWS as the result of either tonic excitatory bombardment occurring during SWS or tonic inhibitory bombardment during alertness or a combination of both (Winson and Abzug, 1978).

Sharpe et al. (1989) found that animals transferred from one environment to another exhibited a substantial increase in EPSPs and large decreases in PSA and latency to peak of PS. Unlike the changes seen by Winson and Abzug (1978), these changes considerably outlasted the behavior that produced them.

Green et al. (1990) had similar results to Sharpe with these new observations: Neither the motor component of exploratory behaviors nor the hippocampal theta rhythm itself was

sufficient to account for the changes in the synaptic and PSA components of the response when animals were introduced into a new environment. Thus, the changes may depend on reorientation of the animal's sensorium during exploration, rather than on movement (Green et al., 1990).

Moser et al. (1993a) and (1993b) later provided evidence that these changes in the EP were most likely brought about by exploration-induced increases in temperature. Later experiments, controlling for temperature, showed long-lasting increases in PSA and EPSP slope during spatial learning in an exploration task (Moser, 1994) as well as more transient PSA potentiation when a rat was placed in a novel holeboard environment or encountered a novel stimulus in a hole (Kitchigina et al., 1997).

1.7 The Locus Coeruleus and Norepinephrine (NE)

While LTP has been widely studied, its physiological relevance has remained somewhat of a mystery as a phenomenon similar to a tetanus does not occur naturally in the nervous system. The search for a connection between LTP and memory has led neuroscientists to investigate the role which monoaminergic projections from the brain stem play in modulation of hippocampal electrical activity (Kobayashi et al., 1974; Loy et al., 1980). I will focus on NE.

The major source of NE to the hippocampus as well as cerebral and cerebellar cortices is the nucleus located in the pons known as the locus coeruleus (LC). The LC is a small dense

13

group of NE-containing cell bodies whose axons constitute the major sources of NE innervation of the hippocampus (Kobayashi et al., 1974; Loy et al., 1980, Aston-Jones and Bloom, 1981a). Fibres from the LC form the dorsal noradrenergic bundle before joining the medial forebrain bundle and subsequently entering the hippocampus (Loy et al., 1980). The densest projection is to the hilar region of the DG while there are less diffuse projections to the molecular and granule cell layers (Loy et al., 1980; Stanton and Sarvey, 1985b; Winson and Dahl, 1985). The highly clustered appearance of this cell group within the pons reinforces the idea that these cells would be activated in concert and LC output would be relatively synchronous (Watabe and Satoh, 1980).

In the awake animal the level of LC firing is a direct function of arousal. Cells fire most slowly during slow wave sleep and increase to higher levels with alert arousal (Foote et al., 1980) which is likely when an animal would learn or form a memory. Furthermore, phasic increases in firing occur to any behaviorally-arousing stimulus in awake animals (Aston-Jones and Bloom, 1981a and 1981b). The firing rate of NE cells is highly dependent upon behavioural state, sensory input from all modalities (Aston Jones and Bloom, 1981b) and changes of significance of environmental stimuli (Sara and Segal, 1991). Also, it has been found that LC neurons fire in a burst when a rat e   es a novel hole in a hole-board environment and when the rat encounters a novel stimulus in a hole (Sara et al., 1994; Vankov et al., 1995) Thus, the conditions which lead to increase in release of NE from the LC onto the hippocampus seem to be similar to those which are involved in the modulation of hippocampal activity mentioned earlier.

14

1.8 Neuromodulatory actions of NE

1.8.1 Exogenous NE

Historically, NE was classified as an inhibitory neurotransmitter (Kety, 1970). More recently, however, there is abundant evidence that NE enhances the signal-to-noise ratio in the neocortex and cerebellum by suppressing spontaneous activity of neurons and enhancing the activity evoked by sensory stimuli. For example Foote et al. (1975) found that iontophoresed NE enhanced neuronal activity in the auditory cortex of the squirrel monkey evoked by species-specific calls. Woodward et al. (1979) found that glutamate-induced excitation and GABA-induced inhibition as well as synaptically-evoked excitation and inhibition of cerebellar Purkinje cells were enhanced by NE. It has also been found that both NE application and presumed NE-release activated by electrical stimulation of LC, enhanced both signal and surround inhibition in visual (Waterhouse et al., 1983) and somatosensory (Waterhouse and Woodward, 1980; Waterhouse et al., 1980) cortices. This suggests that NE is involved in modulation of arousal and attention.

Neuromodulatory effects of NE have also been reported in the hippocampus (Harley, 1987). Unconditioned tones normally inhibit evoked hippocampal unit firing while conditioned tones, signaling food, excite unit firing. With concurrent LC stimulation unconditioned tones produced greater unit inhibition while conditioned tones produced greater unit excitation. Thus, NE also appears to enhance signal-to-noise-ratio in the hippocampus (Segal and Bloom, 1976).

15

Here we will concentrate on NE effects in the hippocampus. Segal and Bloom (1976) recorded the activity of hippocampal pyramidal neurons (HPNs) in the DG in awake, freely-moving rats. Most cells were inhibited by a loud auditory stimulus and by electrical stimulation of LC. Inhibitory responses to the tone were antagonized by drugs interfering with noradrenergic transmission. When LC stimulation was used as the UCS in a classical conditioning paradigm, previous inhibitory responses to the tone were reinstituted and when subthreshold LC stimulation preceded a tone the existing conditioned response to the tone was potentiated. These data suggest that the observed inhibitory response to the tone is modulated by the LC NE pathway and that activation of LC can potentiate hippocampal pyramidal neuron responses to behaviorally-significant conditioned stimuli.

Neuman and Harley (1983) showed that both short and long-term potentiation of the field potential in the DG evoked by stimulation of medial PP fibers could be produced in the absence of tetanus by local iontophoretic application of NE in the anaesthetized rat. In 41 of 54 sites tested, potentiation of PSA was observed while in 16 of these 41 sites the potentiation was long-lasting (i.e. lasting greater than 30 minutes), and like LTP, persisted after the initiating stimulus, in this case NE, was discontinued. The latter is termed NE-induced long-lasting potentiation (NE-LLP). Maximal PSA increases were typically attained 30 minutes after NE application. Given the abundant evidence implicating the hippocampus in learning and memory, investigators have suggested that these short and long-term modulatory actions of NE might play a role in attention and memory processes (Harley, 1987). Harley (1991) suggests that the short-term effect would presumably increase the

16

intensity of sensory input/experience or promote attention to the input while the long-term effect could be viewed as the promotion of memory.

Neuman and Harley (1983) observed no consistent EPSP changes. This is typically the case *in vivo. In vitro* both PSA and EPSP slope increases are seen (Lacaille and Harley, 1985; Stanton and Sarvey, 1987; Dahl and Sarvey, 1989). The induction of NE-potentiation was shown to be β-receptor mediated as NE-LLP can be blocked if a β-blocker is administered prior to NE application (Lacaille and Harley, 1985; Stanton and Sarvey, 1987) but once the NE potentiation has been initiated β-blockers have no effect (Harley and Evans, 1988). Potentiation of PP-EP has also been achieved with the β-agonist isoproterenol (Lacaille and Harley, 1985; Dahl and Sarvey, 1989; Dahl and Li, 1994; Knight et al., 1997; Chaulk and Harley, 1998).

1.8.2 Release of endogenous NE

Endogenous release of NE from LC projections in the hippocampus has also been shown to result in potentiation of the PP- EP in the DG. Endogenous release of NE can be achieved by stimulation of LC neurons.

Potentiation of PP-induced PSA and a decrease in population spike onset latency can be produced by electrical stimulation of the LC (Dahl and Winson, 1985; Assaf et al., 1979; Washburn and Moises, 1989). It was found that systemic propranolol, however, did not always block the effects elicited in the hippocampus by LC electrical stimulation, indicating

17

that the β-receptor may not solely responsible for the potentiation observed with this approach (Harley et al., 1989). A more selective method of inducing endogenous NE release is direct glutaminergic stimulation of the LC. A single pressure ejection of glutamate (100-150 nl) within 300 μm of the LC has been shown to result in reliable potentiation of PSA and in increases in EPSP slope (Harley and Evans, 1988). In another study the potentiation of the DG PP-EP induced by glutaminergic stimulation of the LC is long-lasting in 37% of cases (Harley and Milway, 1986). Systemic administration of propranolol and intra-dentate application of propranolol or timolol significantly attenuates these glutamate-induced effects (Harley and Milway, 1986; Harley and Evans, 1988) while β-blockers administered after glutamate-LC-induced potentiation had no effect on the potentiation. Electrical stimulation in the area of the LC is likely to activate fibers of passage in addition to the intended LC cells, thus recruiting other transmitter systems. This may explain why β-blockers did not significantly attenuate potentiation resulting from electrical stimulation of the LC in Harley et al., 1989.

Potentiation of the DG-EP can also be achieved by electrical stimulation of the nucleus paragigantocellularis (PGi), which is the major input to the LC. Stimulation of PGi with 10 ms 333 Hz trains 20-50 ms prior to PP stimulation resulted in potentiation of the DG PSA with no consistent effects on EPSP slope or PSL (Babstock and Harley, 1992). Systemic administration of propranolol sigificantly attenuated the effects of PGi stimulation on PP-evoked DG-EP's (Babstock and Harley, 1992). PGi stimulation results in activation of LC cells (Ennis and Aston-Jones, 1986) which, in turn potentiate of the DG EP.

18

NE-LLP supports the prediction of Kety (1970) who hypothesised that the aroused states, simulated here by application of exogenous NE or LC stimulation, would induce a 'persistent facilitation' of inputs. For example, an animal attacked by a predator would become aroused and this would presumably increase the probability of the animal forming a memory of the predator and related warning cues as a survival mechanism. This model implies that a pairing of the sensory input with the aroused state may result in a strong memory of the sensory input. Human studies have also suggested that β-adrenergic-mediated arousal promotes long-term memory for informational input (Cahill et al., 1994). Consistent with this hypothesis. Hopkins and Johnson (1984) found in CA3 that when high-frequency train (HFT) stimulation, which did not produce LTP on its own, was paired with NE application, LTP was seen. Furthermore, when a HFT that did produce LTP on its own, was paired with NE, the frequency-induced LTP was prolonged. In addition, Stanton and Sarvey, 1985a have reported that frequency-induced LTP does not occur in the DG following NE depletion.

As an example of an effect of NE on memory in the DG, Kovacs et al. (1979) reported that NE depletion blocked the vasopressin-induced effect of improving retention of a passive-avoidance task. In addition depletion of LC-NE by 6-OHDA in the accessory olfactory bulb abolishes olfactory memory for male mouse odor in the female mouse (Keverne and de la Riva, 1982).

Yet another method of inducing endogenous release of NE and achieving potentiation of the PP-evoked potential is through systemic injection of the α2-adrenoreceptor antagonist idazoxan (IDA). In the anesthetized rat. Richter-Levin et al. (1991) found that systemic IDA (2 mg/kg i.p.) enhanced the population spike of the PP-EP and decreased the field EPSP in the DG. In the awake, freely moving rat. Sara and Bergis (1991) found that systemic IDA (2 mg/kg i.p.) enhanced the population spike of the PP-EP in the DG with no effect on the field EPSP. IDA, via blockade of inhibitory autoreceptors, increases the firing rate of NE-LC neurons (Cedarbaum and Aghajanian. 1978) and increases release of NE in the hippocampus in a dose-dependent manner (Thomas and Holman. 1991).

IDA is a useful method of activation of LC cells and of increasing NE levels to produce NE-related DG-EP potentiation. The Sara lab has found that IDA results in enhanced memory retrieval (Sara and Devauges. 1989). increased behavioral responses to novel objects in a familiar environment and facilitated learning of new response contingencies in a familiar task (Devauges and Sara. 1990) presumably due to its effects on LC-NE.

The previous paragraphs have focused on the effects of NE on the excitatory responses of the principal cells in the DG. How do we study the effects of NE on inhibition or on local circuit interneurons?

1.9 Paired-pulse paradigm

Evoking two PP-EPs in quick succession reveals a change in the response (P2) to the

second pulse relative to the response (P1) to the first pulse (Figure 3). The first pulse enables us to measure the excitatory response of the granule cells and at the same time activates the local hippocampal interneuronal network. By observing P2 we can learn about the modulatory effect which the local network has on the excitatory response. The differences in the resultant response are dependent upon the interval between P1 and P2, called the interstimulus interval (ISI) (DiScenna and Teyler, 1994).

When P2 is smaller than P1, this is referred to as paired-pulse inhibition (PPI) (Joy and Albertson, 1993) (See Figure 3a). The second evoked response is strongly inhibited when stimulation of the PP is spaced by a ISI of approximately 10-20 ms and is inhibited but less strongly when the ISI is between 200-2000 ms (DiScenna and Teyler, 1994). These 2 stages are termed early and late inhibition. PPI is believed to be produced by both feed-forward and feed-back mechanisms (Sloviter, 1987). It has been shown that early inhibition is $GABA_A$-mediated whereas late inhibition is $GABA_B$-mediated (DiScenna and Teyler, 1994).

At an ISI of 40-200 ms P2 is larger than P1. This is called paired-pulse facilitation (PPF) (See Figure 3b) and is thought to be controlled by excitation of granule cells via glutamate receptors of the N-methyl-D-aspartate (NMDA) subtype as it is blocked by NMDA receptor ion channel blockers (Joy and Albertson, 1993).

21

Figure 3

Representative Waveforms from the Results

A. Example of apparent increase in PPI seen after IDA. Waveforms were taken
   from pre-and post-IDA I/O curves on the saline pipette of a single animal.
   (stimulation current = 450 μA)

B. Example of PPF observed at low currents pre-idazoxan. Waveform was taken
   from from pre-IDA I/O curve on the timolol pipette of a single animal.
   (stimulation current=125 μA)

A

Pre-Idazoxan   **Post-Idazoxan**

B

23
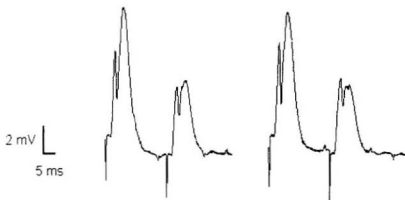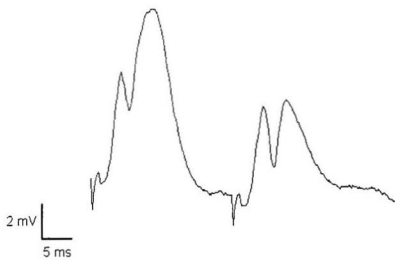
While most paired-pulse work has been carried out in anesthetized animals, it has been found that the characteristics of responses to paired-pulse stimulation in awake rats are dependent on the animal's behavioural state (Austin et al., 1989). In the experiment mentioned above, Sara and Bergis (1991) tested the effect of IDA on enhancement of the PP-evoked DG-EP as well as on PPI of the EP in a two-part study. In the first part of the experiment they found that IDA increased PSA of P1 but had no effect on EPSP slope. This effect was seen in 7 of 8 animals tested and only at currents less than 400 μA. In the second experiment, the effect of IDA on PPI was tested only at currents which evoked a population spike of 50% maximum and for which IDA did not increase PSA (usually 400 μA) in order to ensure that any increase in inhibition seen was not due to the effect of the drug on the first spike. An apparent increase in PPI was seen in 5 of 8 animals. In these the increase in PPI occurred at current intensities at which there was no effect of the drug on the first spike suggesting the increase in inhibition is independent of changes in the size of PSA of P1 and that NE-induced potentiation of P1 and the increase in PPI are separate processes. Sara and Bergis (1991) argue that the effect of IDA on DG cell excitability is dependent on drug-induced release of NE since in a previous study (Richter-Levin et al., 1991) it did not occur when the NE presynaptic terminals were destroyed by the neurotoxin DSP4.

Moser (1996) conducted an experiment using the paired-pulse paradigm with ISIs < 40 ms to investigate the extent to which inhibitory interneurons control impulse flow through the dentate gyrus during spatial learning in exploration of an unfamiliar enviroment. It was found that the EPSP of P2 was reduced further in the exploration condition when compared

24

to P2s with similar P1 sizes in the resting condition. PSA of P2 was facilitated. This suggests that exploration involves increased inhibition on PP terminals or granule cell dendrites while inhibition on the somata is actually decreased (Moser, 1996). Kitchigina et al. (1997) had previously shown that PSA of P1 increase during exploration of a novel environment and that this increase is blocked by a β-blocker.

1.10 The present study

The purpose of the current study was to further explore the modulatory effects of NE in the DG of the dorsal hippocampus. The goals were to:

1) repeat the enhancing effect of IDA on the DG-EP;

2) test local β-blockade on this phenomenon;

3) repeat the effect of IDA on PPI found by Sara and Bergis, 1991 and ensure the observed effect is independent of the effects of NE on P1;

4) explore the role of β-receptor activation on the apparent NE-induced change in inhibition and

5) assess the possibility that NE release might mediate the effects of exploration on dendritic inhibition by looking at PPI of the EPSP slope as well as of PSA.

The study involves the evaluation of the effects of NE on excitation and inhibition of the PP-evoked potential by using systemic administration of the α-2 antagonist IDA to increase NE levels over an extended period and by using the paired-pulse paradigm to probe local-circuit feedback inhibition. In order to explore the pharmacology of the system we used a double pipette technique similar to that employed by Steward et al., 1990.

The logic of the double-pipette technique is illustrated through a study by Steward et al. (1990). They recorded simultaneously from two glass recording micropipettes separated by a distance of 0.5-1.0 mm - one containing saline and the other the GABA antagonist bicuculline - in order to investigate the effects of contralateral commissural stimulation on the PP-EP in the DG. Relatively large openings in the pipette tips ensured that local passive diffusion of drugs from the pipettes could occur. Spread of bicuculline did not extend to the control site as the combined effects of GABA inhibition and commissural stimulation - i.e. multiple spiking and LTP - were only seen at the bicuculline site and not at the saline control site. Recording from the bicucilline site was stable for long periods of time and did not effect the saline recording site indicating a continuous, localized diffusion of drug (Steward et al, 1990).

The double-pipette set-up, while technically more difficult, has many advantages over single pipette recording experiments. Each animal acts as its own internal control as the control (saline) and test (drug) experiments are conducted concurrently. As the two pipettes are recording from the same animal at virtually the same site at the same time, many physiological changes and other variables, which would contribute to interanimal variability,

are the same at both recording sites. Some examples of these variables are temperature, anaesthetic, stimulating electrode placement and ceiling effects. The drug effect is easily determined by a comparison of the control and test sites. The blunt-tip micropipette technique provides a useful alternative to iontophoresis for local drug delivery (Steward et al., 1990).

In the current study, pipettes contain saline and the β-blocker timolol. Thus, effects of local β-receptor block on IDA-induced modulation of the EP can easily be assessed by comparison of the 2 responses after systemic injection of the α2-antagonist. Both pipettes were directed at the dentate gyrus of the left hemisphere of the hippocampus.

2. Methods

2.1 Subjects

Subjects were 15 male Sprague-Dawley rats (Memorial University Vivarium) weighing 250-350g. The experimental protocol conformed to IACC/CCAC guidelines. Each animal was anesthetized with urethane (1.5 g/kg i.p.) and placed skull-flat in a stereotaxic frame. Supplemental doses of urethane were given at 30-minute intervals following the first injection if animals continued to respond to foot pinch. No animal required more than 2 supplements. Core body temperature was maintained at 37 ± 1°C using a rectal probe coupled to a heating pad and temperature control unit. Small holes were drilled in the skull at points referenced from bregma to accommodate electrodes in the DG and PP.

2.2 Electrode placements

A bipolar stimulating electrode (NE100) was placed in the PP of the left hemisphere (7.2 mm posterior, 4.1 mm lateral and 3.0-3.5 mm ventral to brain surface). Recording electrodes were 2 glass micropipettes positioned in the cell body layer or hilus of the dentate gyrus of the dorsal hippocampus (3.5 mm posterior and 2.0 mm lateral to bregma). Exact depths of stimulating and recording electrodes were determined by monitoring of obtained responses. One recording pipette contained 0.9% saline while the second contained 100 μM timolol hydrochloride (Sigma) in 0.9% saline. Inner pipette tip diameters ranged from 40-55 μm while outer diameters were 50-65 μm. Impedances of the pipettes ranged from 1-3 MΩ. In a given experiment, diameters of the 2 pipettes never differed by more than 5 μm and

28

impedances never differed by more than 0.5 MΩ   Both pipettes were held in a Narishige holder which permitted movement of the timolol pipette in 3 dimensions relative to the stationary saline pipette. The timolol pipette was posterolateral to the saline pipette and pipettes were at a distance of 0.5 to 1mm from each other.

2.3 Stimulation and recording of evoked potentials

The 'Workbench' program in the commercial electrophysiological software package 'Brainwave' (Datawave Technologies) was used to control the stimulation and recording parameters in the experiment. Two monophasic 0.2 milliseconds pulses with an inter-stimulus interval (ISI) of 15-30 ms were generated by a Datawave A/D board and delivered through a constant current unit at a frequency of 0.1 hz. Signals were amplified using a bandwidth of 0.1-3.0 Khz by a Grass pre-amplifier and displayed on a dual-channel analogue oscilloscope. Waveforms were digitized on-line at a rate of 10.000 points/ second, displayed on a computer monitor and stored using Brainwave and a PC.

2.4 Experimental protocol

For each subject stimulating electrodes were lowered first. Then, animals received paired-pulse stimulation typically at 200–400 μA current as recording electrodes were lowered to approximate depths of 3.0-3.5 mm below brain surface until maximal PSA was obtained. Position of the recording electrodes were adjusted until responses (P1) to the first pulse on the two pipettes were matched as closely as possible with respect to PSA and each showed

29

population spike latencies of 4 milliseconds or less. ISI was then adjusted until paired-pulse inhibition was observed on both pipettes and until PSA of the second response on each pipette was large enough to be measured.

Initially, an input-output (I/O) curve was obtained, typically beginning at a current of 50 µA and proceeding in 25 µA increments at intervals of 1-minute (6 stimulations) per current value, to the current yielding apparent maximal popspike amplitude as observed on the oscilloscope. I/O curves for each animal consisted of 25-35 different currents.

In the second step stimulation was adjusted to the lowest current at which a measurable PSA was observed in the second response on both pipettes and a 15-minute pre-idazoxan baseline was taken.

In the third step the subject was injected with idazoxan hydrochloride (5 mg/kg i.p.) after which evoked potentials were recorded for approximately 1.5 hours post-drug.

For 8 of the 15 animals, a fourth step was included in the protocol in which a post-idazoxan I/O curve was obtained starting at approximately 1.5 hours post-idazoxan using the same currents as the pre-idazoxan I/O curve.

2.5 *Histology*

Immediately after the recording procedure the subject was removed from the stereotaxic apparatus and decapitated with a guillotine. Within 10 minutes of sacrifice, the brain was removed and frozen in approximately 20 mL of 2-methyl butane which had been

previously cooled in a -80°C freezer for at least 20 minutes. Brains were stored in the same freezer until sectioning.

For easy verification of recording electrode position, brains were cut into 30 µm sections on a Jung Frugocut cryostat microtome and alternate consecutive sections were placed on 2 groups of glass microscope slides. One group was subjected to acetylcholinesterase-metachromatic Nissl staining procedure (Paxinos and Watson, 1986) and the other stained for glycogen phosphorylase (Harley and Bielajew, 1992). The latter stain assisted in localizing the glass pipette tip, the former in identifying cells layers.

2.6 Evoked potential parameter extraction

For each animal the parameter extraction option in the 'Workbench' program was used to measure PSA and EPSP slope. Measurement #25 (Peak to valley) from the 'Electrophysiology' function set was used to obtain PSA while measurement #1 was used to determine EPSP slope. PSL was also measured.

2.7 Statistics

2.7.1 The effect of idazoxan on the response to the first pulse

A paired t-test was carried out in which the mean PSA and EPSP slope measurements for each rat from the response to the first pulse obtained during the 15-minute pre-idazoxan

baseline (90 records) in step 2 of the protocol, were compared to measures in the 15-minute period from 30-minutes-post idazoxan injection to 45-minutes post injection.

In the 8 animals which had post-idazoxan I/O curves in their protocols, comparisons of PSA and EPSP slope measures from the response to the first pulse were also carried out between pre- and post-drug I/O curves. Mean PSA and EPSP slope values were calculated for each current in each of the 2 curves by averaging each of the PSA values from the 6 records obtained at each current. These mean values were averaged over all 8 animals to obtain overall mean responses at each current. Using currents of 150-750 µA, to which all 8 animals were exposed, repeated measures ANOVA was also used to determine differences among means at each current.

2.7.2 The effect of idazoxan on paired-pulse inhibition (P1 overlap pre- and post-Idazoxan)

2.7.2.1 Population spike amplitude

For each pair of recorded responses to paired-pulse stimulation on each pipette, an inhibition ratio (P2/P1) value was calculated by dividing the PSA of the response to the second pulse by that to the first. For each animal inhibition plots were constructed by plotting the inhibition ratio (P2/P1) versus the response to the first pulse (P1). Four plots were generated for each animal; 2 for each recording pipette. One plot was constructed using the records in the pre-idazoxan I/O curve and the 15-minute pre-idazoxan baseline (i.e. before

32

idazoxan injection) for each pipette and a second plot using all records after 30-minutes post-idazoxan injection for each pipette.

Since P2/P1 PSA ratio varies with magnitude of P1, the spreadsheet 'Excel' was used to determine PSA P1 values which were in the area of P1 overlap of the pre-idazoxan and 30-minutes-post-idazoxan inhibition plots. Unpaired t-tests for unequal variances were carried out comparing pre-idazoxan PSA P1 values within this overlap to 30-minute-post-idazoxan value within the overlap. One t-test was done for each of the recording pipettes. If necessary, an approximately equal number of values were removed from the appropriate extremes of each of the pre- and post- inhibition plots with overlapping P1's until PSA P1 values in the pre- and post- plots were not significantly different (i.e. until $p > 0.05$). Then, the P2/P1 values associated with the P1 values remaining after removal of extremes were used to calculate pre- and post-idazoxan P2/P1 means which were subjected to statistical analysis of grouped data in the form of paired t-tests in order to determine if inhibition before idazoxan was significantly different from that after the drug.

2.7.2.2 EPSP slope

Only those slope values that were associated with PSA P1 values in the pre- and post-idazoxan plots that were not significantly different (i.e. until $p > 0.05$) were used in the analysis. Grouped paired t-test analysis were carried out to determine pre- and post-IDA differences in EPSP slope values as was done for PSA P2/P1 ratios above.

2.7.3 The effect of idazoxan and timolol on paired-pulse inhibition at constant current levels
(I/O curves pre- and post-idazoxan)

In the 8 animals which had post-idazoxan I/O curves in their protocols, comparisons of PSA and EPSP slope inhibition measures were carried out between the pre- and post-IDA I/O curves on each pipette for each animal. For each pair of recorded responses to paired-pulse stimulation in each I/O curve on each pipette, an inhibition ratio (P2/P1) value was calculated by dividing the PSA of the response to the second pulse by that of the first. Mean PSA and EPSP slope P2/P1 values were calculated for each current in each of the 2 curves by averaging each of the PSA values from the 6 records obtained at each current. These mean values were averaged over all 8 animals to obtain overall mean responses at each current. Pipette x Drug x Current 3-way repeated measures ANOVAs were used to evaluate differences among means.

2.7.4 Population spike amplitude-to-EPSP slope correlation

PSA -to-EPSP-Slope Pearson correlation coefficients were determined for responses on each pipette using all records pre-idazoxan and all records 30-minutes post-idazoxan and later for each animal for both P1 and P2/P1 ratios.

3. Results

3.1 General

One of the 15 animals was excluded from the analysis because of unexplained abrupt changes in EP parameters. Significant negative P1 to P2/P1 correlations ($p < 0.01$), ranging from -0.11 to -0.78, were found in all but 1 animal confirming the hypothesis that stronger P1s are associated with stronger feedback inhibition and, justifying the use of the P1-matching technique for analysis of PPI, described in the Methods section.

3.2 Histology

A composite drawing of recording electrode placement is provided in Figure 4. Placements were in or near the granule cell layer of the DG or hilus. Although the drawing shows the DG at 3.5 mm posterior to Bregma, the saline electrodes were in reality positioned slightly anterior to this while timolol electrodes were slightly posterior. Timolol pipettes were directed anterolateral to saline pipettes in an attempt to compensate for hippocampus becoming more lateral as one proceeds posteriorly. Despite this, however, timolol placements in the DG were generally more medial than those of saline pipettes. Seven timolol pipettes were placed in the medial hilar apex while the remaining 7, and all 14 saline pipettes, were in the laterodorsal cell blade of dentate gyrus. This placement difference will be addressed in the discussion.
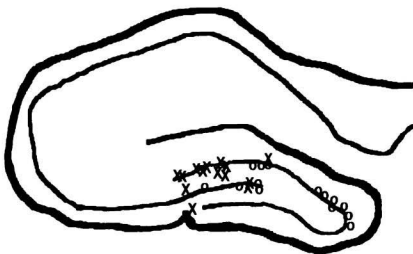
X - Position of saline pipette
O - Position of timolol pipette

Figure 4

**Composite diagram of tranverse section through hippocampus illustrating placement
of saline and timolol recording electrodes in 14 animals**

3.3 Effect of idazoxan on the response to the first pulse (P1)

3.3.1 Effect on population spike amplitude

3.3.1.1 Fifteen- minute recording pre- and post-idazoxan

Mean baseline PSA (Figure 5A) for the saline pipette (n=14) was 4.37 mV; mean baseline PSA for the timolol pipette was 5.19 mV. This difference was significant (paired t-test; t_{13}=3.36; p<0.01). Following IDA, as predicted, PSA on the saline pipette was significantly increased to 116 % of baseline (paired t-test; t_{13}=5.89; p<0.01). On the timolol pipette the increase (108%) was not significant (paired t-test; t_{13}=1.11; p>0.05).

3.3.1.2 I/O Curves pre- and post idazoxan

Figures 6 and 7 show PSA means obtained using pre- and post-idazoxan I/O curves (n=8) for each current for the saline and timolol pipettes separately. Pipette x idazoxan x current (2 x 2 x 25) repeated measures ANOVA revealed a significant main effect of current ($F_{24,168}$=8.99; p<0.0001) on PSA as well as a significant IDA x current interaction ($F_{24,168}$=2.04; p<0.01). Newman-Keuls post-hoc comparisons at P=0.05 showed that IDA significantly increased PSA for currents ranging from 175-475 µA. Since potentiation of PSA was observed only on the saline pipette in the fifteen- minute recording pre- and post-IDA and on both pipettes in the I/O curve 3-way ANOVA, separate two way ANOVAs were carried out for each pipette. This analysis showed that significant potentiation occurred on the saline pipette ($F_{1,24}$=13.19; p<0.05) while there was no significant potentiation on the timolol

Figure 5

Effect of Idazoxan on the response to the first pulse (P1) (15-minute intervals)

A. **PSA:** Mean P1 PSA (± S.E.M) across animals is shown for saline and timolol pipettes pre- and post-idazoxan. $N = 14$

B. **EPSP slope:** Mean P1 EPSP slope (± S.E.M) across animals is shown for saline and timolol pipettes pre- and post-idazoxan. $N = 14$

C. **PSL:** Mean P1 PSL (± S.E.M) across animals is shown for saline and timolol pipettes pre- and post-idazoxan. $N = 14$

A

Population Spike Amplitude (mV)

Saline Pipette   Timolol Pipette

Pre-Idazoxan
Post-Idazoxan

B

EPSP Slope (mV/ms)

Saline Pipette   Timolol Pipette

Pre-Idazoxan
Post-Idazoxan

C

Population Spike Latency (ms)

Saline Pipette   Timolol Pipette

Pre-Idazoxan
Post-Idazoxan

39
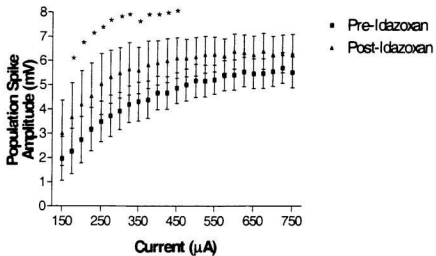
Figure 6

Effect of Idazoxan on PSA of the response to the first pulse (P1) on saline pipette. Mean P1 PSA (± S.E.M) across animals is shown for each current in pre- and post-idazoxan I/O curves. $N = 8$

Figure 7

Effect of Idazoxan on PSA of the response to the first pulse (P1) on timolol pipette. Mean P1 PSA (± S.E.M) across animals is shown for each current in pre- and post-idazoxan I/O curves. $N = 8$

pipette ($F_{1,24}$=0.17; p>0.05), in agreement with the 15-minute analysis.

3.3.2 Effect on EPSP slope

3.3.2.1 15-Minute recording pre- and post-idazoxan

Mean baseline EPSP slope (Figure 5B) for the saline pipette (n=14) was 5.08 mV/ms. Mean baseline EPSP slope for the timolol pipette was 6.04 mV/ms. This difference was not significant (paired t-test; t_{13}=1.72; p>0.1) Following idazoxan there was no change in EPSP slope on either the saline (paired t-test; t_{13} = 0.574; p>0.05) or the timolol pipette (paired t-test; t_{13} =1.63; p>0.05). Post-IDA EPSP slope size averaged 98% of baseline on the saline pipette and 93% of baseline on the timolol pipette.

3.3.2.2 I/O curves pre- and post-idazoxan

Figures 8 and 9 show EPSP slope means obtained using pre- and post-idazoxan I/O curves (n=8) for each current for the saline and timolol pipettes separately. Pipette x IDA x current (2 x 2 x 25) repeated measures ANOVA showed significant effects of current ($F_{24,168}$=5.52; p<0.05) and idazoxan ($F_{1,7}$=5.70; p<0.001) as well as a significant idazoxan x current interaction ($F_{24,168}$=2.16, p<0.01). Newman-Keuls post-hoc comparisons
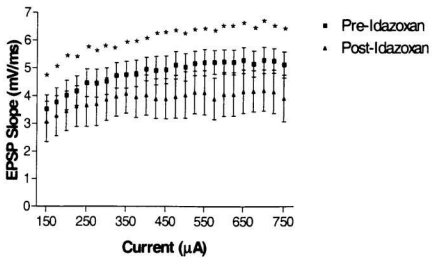
Figure 8

Effect of Idazoxan on EPSP slope of the response to the first pulse (P1) on the saline pipette. Mean P1 EPSP slope (± S.E.M) across animals is shown for each current in pre- and post-idazoxan I/O curves. $N = 8$
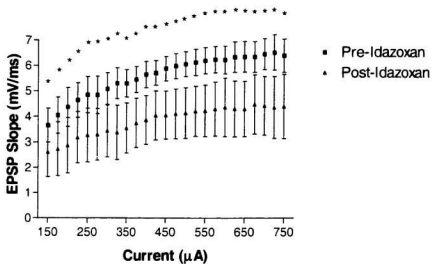
Figure 9

Effect of Idazoxan on EPSP slope of the response to the first pulse (P1) on the timolol pipette. Mean P1 EPSP slope (± S.E.M) across animals is shown for each current in pre- and post-idazoxan I/O curves. $N = 8$

at $P=0.05$ showed that IDA significantly decreased EPSP slope at all current levels (150-750 µA).

3.3.3 Effect on population spike latency

3.3.3.1 15-Minute recording pre- and post-idazoxan

Mean baseline P1 PSL (Figure 5C) for the saline pipette (n=14) was 3.86 ms; mean baseline P1 PSL for the timolol pipette was 3.91 ms. Following IDA there was no significant change in P1 PSL on either the saline (paired t-test; $t_{13}= 0.062$; p>0.05) or the timolol pipette (paired t-test; $t_{13} =0.913$; p>0.05). Post-idazoxan P1 PSL means were 3.86 ms on the saline pipette and 3.69 ms on the timolol pipette.

3.3.3.2 I/O curves pre- and post-idazoxan

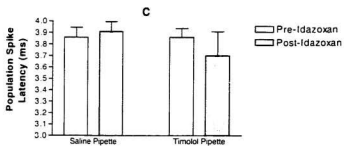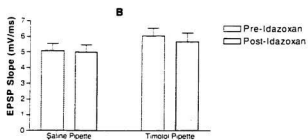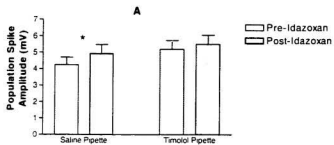Figures 10 and 11 show population spike latency means obtained using pre- and post-idazoxan I/O curves (n=8) for each current for the saline and timolol pipettes separately. Pipette x idazoxan x current repeated measures ANOVA showed only a significant effect of current on population spike latency ($F_{24,168}=8.07$; p<0.0001). Stronger currents reduced population spike latency.

3.4 Effect of idazoxan on paired-pulse inhibition
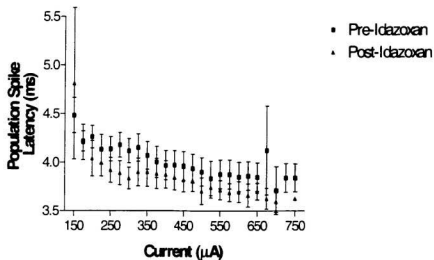
Figure 10

Effect of Idazoxan on PSL of the response to the first pulse (P1) on the saline pipette. Mean P1 PSL (± S.E.M) across animals is shown for each current in pre- and post-idazoxan I/O curves. $N = 8$
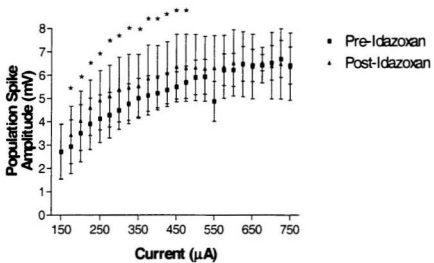
Figure 11

Effect of Idazoxan on PSL of the response to the first pulse (P1) on the timolol pipette. Mean P1 PSL (± S.E.M) across animals is shown for each current in pre- and post-idazoxan I/O curves. $N = 8$

3.4.1 Effect on population spike amplitude

3.4.1.1 Effect of idazoxan on paired-pulse inhibition using P2/P1 values associated with
overlapping P1 values that were not significantly different pre- and post-idazoxan

Figure 12 shows mean P2/P1 PSA ratio pre- and post-idazoxan for saline and timolol
pipettes seperately (n=14). Mean baseline P2/P1 PSA ratio on the saline pipette was 0.481;
mean baseline P2/P1 PSA ratio on the timolol pipette was 0.614. This difference was not
significant (paired t-test; t_{13}=1.72; p>0.1). P1 mean on the saline pipette was 4.72 mV (mean
number of records = 233) while P1 mean on the timolol pipette was 5.31 mV (mean number
of records = 242). Following IDA. ratios decreased to 0.376 on the saline pipette (paired
t-test; t_{13}=3.71 . p<0.01) and to 0.471 on the timolol pipette (paired t-test; t_{13}= 3.17; p<0.01)
indicating increases in inhibition on both pipettes. P1 mean on the saline pipette was 4.67 mV
(mean number of records = 328) while P1 mean on the timolol pipette was 5.43 mV (mean
number of records = 315).

3.4.1.2 Effect of idazoxan and timolol on paired-pulse inhibition at constant current levels

Figures 14 and 15 compare mean P2/P1 population spike amplitude ratios obtained
using pre- and post-idazoxan I/O curves (n=8) for each current for the saline and timolol
pipettes separately. PPF can be seen at lower currents. Although there was a lot of

Figure 12

Effect of Idazoxan on paired-pulse inhibition of PSA on saline pipette and timolol pipettes. Mean P2/P1 PSA ratio for analysis matched for P1 PSA (± S.E.M) averaged across animals is shown. $N = 14$ A significant decrease in P2/P1 PSA ratios (i.e. increase in inhibition) was seen on both pipettes.

Figure 13

Effect of Idazoxan on paired-pulse inhibition of EPSP slope on saline and timolol pipettes. Mean P2/P1 EPSP slope ratio for analysis matched for P1 PSA (± S.E.M) averaged across animals is shown. $N = 14$ A significant decrease in P2/P1 EPSP slope ratios (i.e. increase in inhibition) was seen on the timolol pipette but not on the saline pipette.

Figure 14

Effect of Idazoxan on paired-pulse inhibition of PSA on the saline pipette. Mean P2/P1 PSA ratio (± S.E.M) across animals is shown for each current in pre- and post-idazoxan I/O curves. $N = 8$

Figure 15

Effect of Idazoxan on paired-pulse inhibition of PSA on the timolol pipette. Mean P2/P1 PSA ratio (± S.E.M) across animals is shown for each current in pre- and post-idazoxan I/O curves. $N = 8$

variation in responses at lower current prior to IDA all animals showed some degree of PPF pre-IDA at lower currents (Figure 3 B).

Repeated measures ANOVA showed that there was a significant idazoxan x current interaction ($F_{24,104}$ =4.19; p<0.0001). Newman-Keuls post-hoc comparisons P=0.05 showed that IDA actually caused a reduction of a facilitation (rather than an increase in inhibition) of PSA P2/P1 ratio at currents of 150 and 175 uA (Figure 3A).

3.4.2 Effect on EPSP slope

3.4.2.1 Effect of idazoxan on paired-pulse inhibition using P2/P1 values associated with overlapping P1 values that were not significantly different pre- and post-idazoxan

Figure 13 shows the mean P2/P1 EPSP slope ratio for pre- and post-idazoxan for both pipettes (n=14). Mean baseline P2/P1 EPSP slope ratio for the saline pipette was 0.730 ; mean baseline P2/P1 EPSP slope ratio for the timolol pipette was 0.721. This difference was not significant (paired t-test: t_{13}=0.45; p>0.5). P1 mean on the saline pipette was 5.39 mV/ms while P1 mean on the timolol pipette was 6.05 mV/ms. Following IDA, P2/P1 EPSP slope ratio on the timolol pipette was significantly decreased to 0.653 (paired t-test: t_{13}=2.59, p<0.05) indicating an increase in inhibition. There was no corresponding change on the saline pipette (paired t-test: t_{13}= , p>0.05) where post-IDA the P2/P1 EPSP slope ratio was 0.718. Post-IDA P1 mean on the saline pipette was 4.68 mV while P1 mean on the timolol pipette was 5.18 mV.

53

3.4.2.2 Effect of idazoxan and timolol on paired-pulse inhibition at constant current levels

Figures 16 and 17 compare mean P2/P1 EPSP slope ratios obtained using pre- and post-IDA I/O curves (n=8) for each current for the saline and timolol pipettes separately.

Repeated measures ANOVA showed that there was a significant main effect of idazoxan in decreasing EPSP slope P2/P1 ratio ($F_{1,7}$=17.4; p<0.01) as well as a significant main effect of current ($F_{2,14}$=1.63; p<0.05).

3.4.3 Effect on population spike latency

3.4.3.1 Effect of idazoxan on paired-pulse inhibition using P2/P1 values associated with overlapping P1 values that were not significantly different pre- and post-idazoxan

Mean baseline P2 PSL for the saline pipette (n=14) was 4.79 ms; mean baseline P2 PSL for the timolol pipette was 4.62 ms. Following idazoxan there was no significant change in PSL on either the saline (paired t-test; t_{13} =-0.483; p>0.05) or the timolol pipette (paired t-test; t_{13} =-0.198; p>0.05). Post-IDA PSL means were 4.82 ms on the saline pipette and 4.64 ms on the timolol pipette.

3.4.3.2 Effect of idazoxan and timolol on paired-pulse inhibition at constant current levels
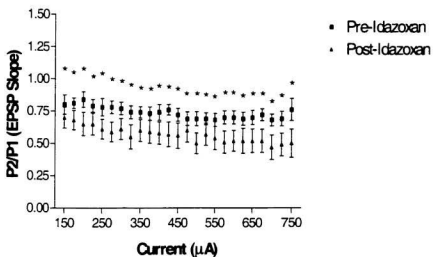
Figure 16

Effect of Idazoxan on paired-pulse inhibition of EPSP slope on the saline pipette. Mean P2/P1 EPSP slope ratio (± S.E.M) across animals is shown for each current in pre- and post-idazoxan I/O curves. $N = 8$
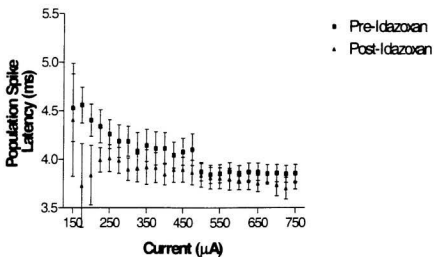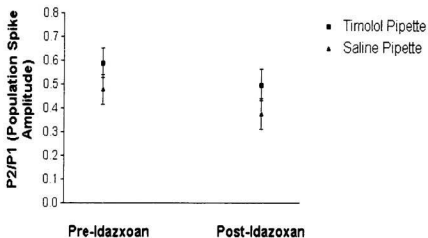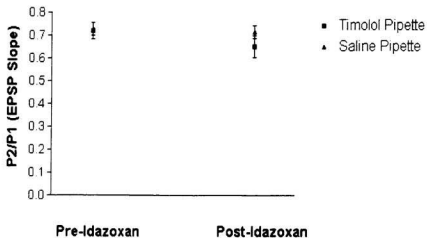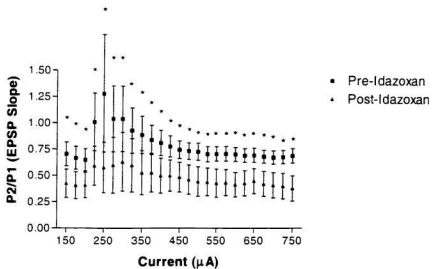
Figure 17

Effect of Idazoxan on paired-pulse inhibition of EPSP slope on the timolol pipette. Mean P2/P1 EPSP slope ratio (± S.E.M) across animals is shown for each current in pre- and post-idazoxan I/O curves. $N = 8$

Figure 18 and 19 compare mean P2/P1 population spike latency ratios obtained using saline and timolol pipette I/O curves averaged over the 8 animals for each current pre- and post-idazoxan separately. Pipette x IDA x current repeated measures ANOVA showed only a significant main effect of increasing current levels in decreasing P2/P1 ($F_{24,168}=8.07$; $p<0.0001$) population spike latency ratio.

3.5 Population spike amplitude-EPSP slope correlations

3.5.1 P1

On both the saline and timolol pipettes there were significant positive correlations between population spike amplitude and EPSP slope in each animal (n=14) pre-idazoxan ($p<0.01$) and in all but 1 animal post-IDA ($p<0.01$). Correlation magnitude grew smaller after IDA administration on both pipettes in all animals. Overall, mean correlations were 0.777 pre-IDA and 0.430 post-IDA for the saline pipette and 0.792 pre-IDA and 0.499 post-IDA for the timolol pipette. Overall, correlations were significantly lower after IDA than before on both the saline (paired t-test; t= 5.69; df=13; $p<0.0001$) and timolol (paired t-test; t=3.67; df=13; p=0.01) pipettes.

3.5.2 P2/P1 ratio

There were no significant correlations between PSA P2/P1 ratio and EPSP slope P2/P1 ratio pre- or post-IDA on either pipette ($p>0.05$) in any animal (n=14). Over
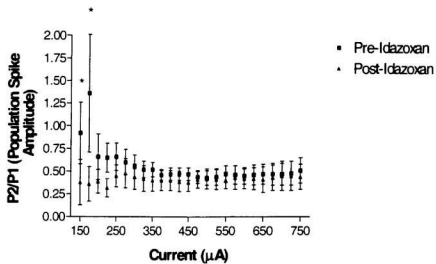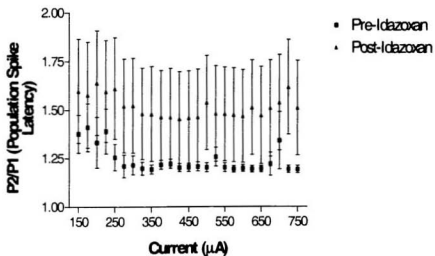
Figure 18

Effect of Idazoxan on paired-pulse inhibition of PSL on the saline pipette. Mean P2/P1 PSL ratio (± S.E.M) across animals is shown for each current in pre- and post-idazoxan I/O curves. $N = 8$
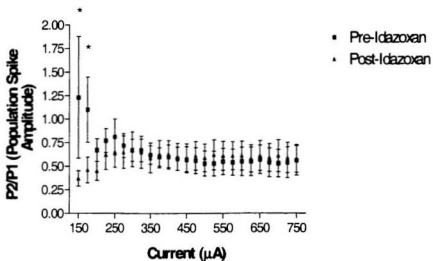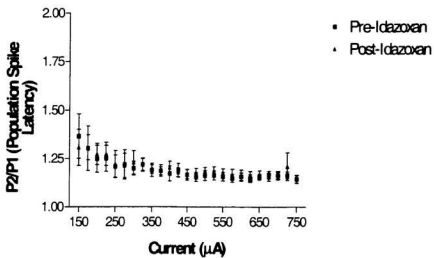
Figure 19

Effect of Idazoxan on paired-pulse inhibition of PSL on the timolol pipette. Mean P2/P1 PSL ratio (± S.E.M) across animals is shown for each current in pre- and post-idazoxan I/O curves. $N = 8$

all 14 animals, mean correlations were 0.064 pre-idazoxan and 0.062 post-idazoxan for the saline pipette and 0.266 pre-idazoxan and 0.148 post-idazoxan for the timolol pipette. There were no significant differences in correlations pre- and post-idazoxan on either the saline (paired t-test: t=0.025; df=13; p>0.05) or the timolol (paired t-test: t=1.26; df=13; p>0.05) pipette.

4. Discussion

4.1 Effect of timolol on baseline response (P1)

Seven timolol pipettes were placed in the medial hilar apex while the remaining 7, and all 14 saline pipettes, were in the laterodorsal cell blade of dentate gyrus. An analysis of pipette placement x drug pipette did not show an effect of placement ($F_{1,12}=0.00$; $p>0.05$) but only of timolol itself ($F_{1,12}=10.89$; $p<0.05$). Thus, although the difference was small (0.9-1 mV), there was a consistently larger spike from pipettes containing the β-receptor antagonist. Tonic blockade of β-receptors may result in an enhanced PSA for a given input, possibly by reducing the activity of tonically or feed-forward activated interneurons.

Rose and Pang (1989) have shown tonically active interneurons near the cell body layer of dentate gyrus are excited by β-receptor activation. Other studies also report larger PSA following 6-OHDA depletion of NE (Robinson and Racine, 1985; Robinson et al., 1993). Finally, Winson and Dahl (1985) showed that iontophoresis of sotalol, another β-receptor antagonist, also increased PSA at the cell body layer. These results all support the present observation.

In contrast, Bliss et al. (1983) found that NE-depletion *in vivo* with 6-OHDA did not effect excitability of granule cells. *In vitro* studies have not reported increased medial PP spike size with perfusion of timolol (Lacaille and Harley, 1985) or metoprolol (Stanton and

Sarvey, 1985b). However, Pelletier et al. (1994) did see increased lateral PP PSA and decreased medial PP PSA with perfusion of metoprolol. Systemic β-blockade *in vivo* also does not increase, and may decrease PSA size (Babstock and Harley, 1992). However, *in vitro* results may be affected by the abnormal status of inhibitory systems in the slice and systemic β-receptor antagonism would affect heart rate and other systemic variables that might depress responses and mask small changes in somatic inhibition. More closely related is an earlier study with 7 rats using timolol or propranolol in a similar two-pipette experiment (Munro et al. 2001). No significant difference in spike size was reported. However, in this study, timolol concentrations used varied from 10 to 50 μM while the present study used 100 μM.

The PSA difference between pipettes in the present study did not reach significance in a 3-way ANOVA on the smaller set of I/O curve data although the direction of difference is the same (see Figures 6 and 7). Thus, the positive results favoring a role for β-receptors in mediating inhibitory effects of basal levels of NE in dentate gyrus is only suggestive and further experimentation will be needed. The main strength of this result is its correspondence with interneuron recording evidence that β-receptor activation increases firing in a somatic subpopulation of GABAergic interneurons.

4.2 Effect of Idazoxan on P1

4.2.1 Effect on population spike amplitude

IDA (5 mg/kg i.p.) resulted in an increase in PSA of the EP in the dorsal DG similar to that demonstrated by Sara and Bergis (1991) and Richter-Levin et al. (1991) with IDA (2 mg/kg i.p.). Enhanced activation of the LC-NE system by IDA produced a significant increase in PSA size that also appeared to depend on β-receptor activation. The PSA increase was seen in both the 15-minute and I/O curve analyses. In the latter analysis PSA was only significantly increased at currents in the 175–475 μA range. Again this follows the pattern seen by Sara and Bergis, 1991, which occurred only at currents less than 400 μA.

It is likely that the IDA effect is mediated by an increase in the basal firing of LC-NE neurons and in reduced autoreceptor inhibition at NE terminals that together produce an increase the release of NE at DG synapses. Richter-Levin et al. (1991) found that IDA-induced potentiation was absent after destruction of LC-NE neurons by application of the NE neurotoxin DSP-4. There is evidence that IDA can bring about an increase in firing of LC neurons by blockade of α2 inhibitory autoreceptors that exist in the LC (Cedarbaum and Aghajanian, 1978) and in the hippocampus (Unerstall et al., 1984). More recent evidence suggests that IDA, which is structurally similar to the imidazolines (Bousquet et al., 1992), increases the firing rate of LC neurons mainly through actions on imidazoline receptors rather than by α2-receptor blockade (Ugedo et al., 1998).

Regardless of the mechanism by which IDA induces increased LC activity, it has been shown that IDA increases the release of NE in the hippocampus (Thomas and Holman, 1991). In this study, 5 mg/kg IDA increased NE levels by approximately 100% over a 75-minute

63

period. NE-mediated PSA potentiation in the DG has been reported many times since its initial description in 1983 (Neuman and Harley) and pharmacological studies have consistently implicated the β-receptor in this increase both *in vitro* (Lacaille and Harley, 1985; Stanton and Sarvey, 1985a and b) and *in vivo* (Harley and Milway, 1986; Harley and Evans, 1988; Babstock and Harley, 1992).

Since, in previous IDA experiments, the PSA potentiation effect was clearest at low currents, a ceiling effect on the timolol pipette is not a likely explanation for the loss of potentiation with β-receptor antagonism in the present study. Although, the 3-way ANOVA on the P1 I/O curve data showed that IDA increased the PSA on both pipettes, separate two way ANOVAs on each pipette showed that significant potentiation only occurred on the saline pipette whereas there was no significant potentiation on the timolol pipette, even at low currents that resulted in similar PSA magnitudes. The convergence with data from other ways of manipulating NE, including direct application and synaptic release of NE, and other ways of producing β-blockade, including other antagonists and direct and systemic applications, argues strongly for a role for NE in the PSA potentiation. The ability of β-receptor blockade at the DG cell layer to attenuate LC-NE or NE-evoked potentiation of perforant path PSA agrees with other results using β-receptor blockade locally or systemically in both *in vivo* and *in vitro* NE studies (Harley and Evans, 1985; Lacaille and Harley, 1985; Stanton and Sarvey, 1985b; Harley and Milway, 1986; Chaulk and Harley, 1998).

A direct effect of β-receptor activation on granule cells may be the most parsimonious

explanation of the apparent β-receptor-mediated NE-induced increase in PSA of P1 in the present study, although a disinhibitory effect is not ruled out. In an earlier paper, another α2-antagonist, rauwolscine, decreases interneuron activity (Pang and Rose, 1987). Through intracellular recording from granule cells, Lacaille and Schwartzkroin (1988) and later, Stanton et al. (1989) reported a β-receptor-mediated, mild but prolonged depolarization of the granule cell membranes accompanied by an increase in membrane resistance which they attributed to a blocking of a potassium conductance activated at resting membrane potential. Thus, in the presence of NE, granule cells would be more depolarised, and inputs would be more effectively transmitted, producing an increased likelihood of cell firing through both effects and thus greater PSA. This PSA enhancement effect might only be activated at suprabasal NE levels in contrast to a possible basal NE promotion of interneuron activity that reduces cell firing. The potentiation of PSA seems to be a higher threshold effect than the difference in baseline already discussed.

4.2.2 Effects on P1 EPSP slope

In the I/O curve analysis there was clear evidence of a decrease in EPSP slope following IDA. This was not seen in the data set comparing the 15-minute period before IDA to one 30 min after IDA. There was no effect of timolol on the decrease in slope. Decreases in EPSP slope with NE have been reported in other *in vivo* experiments, but so have increases and no changes (Lacaille and Harley, 1985; Harley and Milway, 1986; Sara and Bergis, 1991;

65

Chaulk and Harley, 1998). Thus it is uncertain whether this is a typical NE effect. A consistent decrease in slope with IDA was reported in an earlier study (Richter-Livin et al., 1991), however, and this may be related more closely to IDA, which could affect hippocampal imidazoline receptors directly.

On the other hand, Winson and Dahl (1985) reported a decrease in EPSP slope as a reliable effect when iontophoresing NE in the dentate gyrus molecular layer. Any interpretation of slope effects with NE is complicated by the more recently acknowledged differential effect of NE on medial and lateral perforant path input. NE enhances PSA and EPSP slope from the medial PP. NE depresses PSA and EPSP slope from the lateral PP (Dahl and Sarvey, 1989). In the present study latency data suggest all spikes were medial PP spikes, but the angular bundle electrode placements would have excited both medial and lateral synaptic input, thus a predominance of lateral synaptic input in the EPSP slope measure of the 8 rats used in the I/O analysis, for example, might have given rise to the significant decrease observed. This could also account for the occurrence of an apparent slope decrease (lateral PP) coupled with a spike increase (medial PP) under the influence of NE. Increase in the PSA at the same current level with no increase or a decrease in EPSP slope may also be evidence that NE improves EPSP-population spike coupling, with the same synaptic input producing more cell firing in the presence of NE (Sara and Bergis, 1991).

The mechanism for the lateral PP selective slope decrease has not been identified. There are numerous interneuron subtypes in the dentate gyrus and other data from our

66

laboratory suggests NE release can excite, inhibit or not affect interneurons depending on their subtype (Clarke, 1995). Thus the EPSP slope inhibition may be an indirect effect of recruiting a population of interneurons with axonal arbors restricted to the outer molecular layer thus producing dendritic inhibition. Alternatively, presynaptic NE heteroreceptors might mediate such differential modulation. Although there was no significant difference in EPSP slope between pipettes, EPSP slope decreases were, if anything, greater on the timolol pipette pointing toward a possible α1-receptor-mediated depressive effect on EPSP slope. On the other hand, as mentioned, since this effect has been seen previously with idazoxan it may be due to imidazoline effects rather than NE. The detailed location of imidazoline receptors present in the hippocampus has not been described (Kamisaki et al., 1990).

4.3 Effect of idazoxan on paired-pulse inhibition (P2/P1)

4.3.1 Effects on population spike amplitude

Analysis for matched P1 values showed an increase in PPI of PSA in apparent agreement with the results of Sara and Bergis, 1991. However, analysis by current showed that, pre-IDA, there was actually an enhancement of the PSA (i.e. PPF) (Figure 3B) at the lowest two currents (150 and 175 μA) and IDA reduced this enhancement at these currents. There was no difference in feedback inhibition at higher currents. There was variation in responses at low currents prior to IDA administration, however, all animals showed some degree of pre-IDA PPF at one or more of the lowest five currents which was absent post-

67

IDA. Similar effects were observed on both pipettes so it was not clear which receptor might have been involved in the effect.

Sara and Bergis (1991) state that the NE-induced increase in PPI which they observed was surprising given disinhibitory effects of NE reported in CA1 by Mueller et al. (1981). Given this, the authors argued different mechanisms producing opposite effects would likely be required to produce the increase seen in PI and the increase in inhibition seen with the paired-pulse paradigm (Sara and Bergis, 1991). In the present study, we did not observe an increase in inhibition, but a decrease in a facilitatory process, which was present before IDA activated the LC-NE input. Nonetheless, the loss of PPF in the presence of PI facilitation with IDA still argues for distinct mechanisms.

Sloviter (1991) reported a similar PPF of the PSA even in the absence of a population spike associated with the first response. In the present study, PPF was observed at low currents when no population spike or a small population spike only was associated with the first response. We have considered two kinds of explanations for this early facilitation: 1. Paired pulse enhancement of calcium loading in the synaptic terminals favoring increased cell firing to a second pulse before overriding feedback inhibitory circuitry is strongly engaged. 2. Small spikes differentially recruit a disinhibiting subpopulation of interneurons, while larger spikes also engage higher threshold feedback inhibition.

With respect to the first hypothesis, Stanton and Heinemann (1986) have shown no change in molecular layer calcium fluxes with NE although cell layer fluxes increase, which

suggests terminal calcium entry may not be affected by NE. Thus, the disinhibitory interneuron hypothesis is favored here although there is, as yet, no direct evidence.

Sayin et al. (2000) have recently shown that activation of $GABA_B$ autoreceptors can produce PPF of the PSA in the DG at intervals that normally exhibit PPI. If $GABA_B$ autoreceptor activation occurs at lower levels of GABA release, such an effect could play a role in the PPF observed here and in other studies at low currents without invoking a separate disinhibitory population. As a second alternative to disinhibition, NE may be acting on excitatory feedback mossy cells causing an increase in their activity and resulting in a net facilitation of granule cell PSA.

In the matched P1 analysis, average stimulation current over all 14 animals during the main phase of the experiment was approximately 275 µA with currents ranging from 125 to 500 µA. The fact that low currents were used in the matched analysis may explain why this analysis appeared to also indicate a post-IDA increase in PPI. In the I/O curve analysis (Figure 15) one can see that pre- and post-IDA inhibition is almost identical at currents of 300 µA and higher while at around 250-275 µA (about the mean current for the matched analysis) the P2/P1 ratio magnitude is lower after IDA administration.

In sum, a modulation of somatic disinhibitory circuits is favored over direct presynaptic effects. The data do not suggest an increase in feedback inhibition per se.

69

4.3.2 Effects on EPSP Slope

Analysis of matched P1 values showed that IDA increased PPI of the EPSP slope on the timolol pipette, but not on the saline pipette, suggesting that activation of α1–adrenoreceptors may mediate feedback dendritic inhibition. In the I/O curve analysis (n=8), however, there was an increase in PPI of EPSP slope on both pipettes with IDA. Sara and Bergis (1991) did not look at PPI of EPSP slope. This is actually the first report of feedback inhibition of EPSP slope being enhanced by IDA.

The evidence for EPSP facilitation itself is weak in the present data set. EPSP facilitation is not observed at the lowest currents on either pipette, although it does appear at one current on the timolol pipette. The medial perforant path terminals are high release terminals that do not typically show facilitation (McNaughton, 1980). However, as mentioned, NE preferentially enhances medial perforant path input while depressing lateral perforant path input (Dahl and Sarvey, 1989) with effects both on EPSP slope and spike in each case. A higher proportion of lateral PP fibers is one possible mechanism that may account for the observed depression of P1 EPSP slope.

The observed increase in PPI of the EPSP slope with IDA is novel, but relates well to the recent report of the effect of exploration in a novel environment on EPSP slope PPI in dentate gyrus. Moeser (1996) found that PPI of EPSP slope was increased during exploration compared to the control condition at short ISIs. The observed EPSP slope effect required that a population spike be elicited on the first response. This is evidence that the

increase in PPI of EPSP slope resulted from an increase in feedback dendritic inhibition involving an increase in activity of dendritic inhibitory interneurons after their activation by the first pulse. It was not possible to determine if the EPSP effect in the present study required a population spike on the first response because P1s having no population spike were rare especially after IDA application. Moeser suggests the exploration-induced increase in PPI of EPSP which he observed is attributable to an increase in inhibition at PP terminals or granule cell dendrites.

The observed increase in PPI of EPSP slope is not accounted for by the mechanisms offered previously to explain the effects of IDA on P1 (direct granule cell membrane effects) or on the change in P2/P1 PSA (removal of feedback disinhibition at low currents) seen in the present study and therefore must be explained by a separate mechanism. As suggested by Moser, we propose that feedback interneurons synapsing on the granule cell dendrites and increasing dendritic inhibition are also selectively recruited by NE activation. The apparently separate and distinct effects of NE on granule cells and interneuron subpopulations suggested by the present pattern of results would predict a dissociation of the normal EPSP slope/ PSA relationship. That seems to be the case.

4.3.3 Effects on population spike amplitude-to-EPSP slope correlation

The P1 EPSP slope to PSA correlations which were seen pre-IDA were lower after IDA application indicating that there was no post-IDA relationship between PSA and EPSP

71

slope and that effects of NE on these two parameters are likely to be distinct.

4.4 Comparisons with naturalistic observation of DG-EP and altering of noradrenergic transmission during exploration/new environment.

Experiments controlling for temperature, show long-lasting increases in PSA and EPSP slope during spatial learning in an exploration task (Moser, 1994). Other experiments have shown β-receptor-sensitive transient PSA potentiation when a rat is placed in a novel holeboard environment or encountered a novel stimulus in a familiar holeboard environment (Kitchigina et al., 1997). The later experiments were initiated because of the evidence that LC neurons fire in a burst when a rat explores a novel hole in a holeboard environment and when the rat encounters a novel stimulus in a hole. This LC novelty response habituates rapidly (Sara et al., 1994; Vankov et al., 1995). The fact that LC bursts happen with a similar time course to hippocampal PSA changes and that both occur with novel encounters during exploratory behaviour, combined with the finding that DG PSA increases are brought about by LC activation and blocked by β-blockers, provides strong evidence that the LC-NE system mediates this behaviour-dependent gating in the hippocampus (Kitchigina et al., 1997). In addition, in a related study, rats in a holeboard spent more time in contact with holes containing novel objects than with empty holes and this behaviour was enhanced by IDA and decreased by a β-antagonist or by the α2-agonist clonidine (Sara et al., 1995).

In the present study, in an anesthetized preparation the NE-enhancing drug, IDA

72

produced an increase in PSA, which was attenuated by a β-blocker, adding to the evidence that the LC-NE system mediates enhancement in information transmission in the hippocampus through the β-receptor, changes which may be behaviourally dependent in the awake animal.

In addition, as previously stated, Moser (1996) found an increase in PPI of EPSP slope during exploration relative to the control condition. Similarly, in the present study IDA resulted in an increase in PPI of EPSP slope as in Moser's exploration condition. To my knowledge, this is the first observation of NE modulation of PPI of EPSP slope. The result suggests that LC-NE may also be the neurotransmitter involved in increasing dendritic inhibition during exploration. This can be readily tested, perhaps by using α-blockers, as evidence from the present study suggests that these effects may be α1-receptor mediated.

Opposite to effects on PPI of EPSP slope, Moser (1996) found a decrease in PPI of PSA during exploration while, in the present study, IDA resulted in a decrease in a facilitatory contribution. This suggests that a different neurotransmitter is involved in the exploration-triggered decrease in PPI that Moser found for PSA.

4.5 Proposed Model Explaining Results

Figure 20 illustrates a proposed model of the effects of LC-NE on granule cells and interneurons in the DG. In summary, there are five main results in the present study suggesting five distinct roles for the neuromodulator NE in local circuit operations in the DG.

73

Each will be considered in turn.

1) First, at baseline, low threshold b-receptor activation enhances tonic activity of somatic inhibitory interneurons. Interneurons, probably basket cells, represented by interneuron A, which synapse on the cell bodies of granule cells, fire tonically, at a constant rate thus playing a role in determining baseline response of granule cells. Significantly larger P1 population spikes seen on timolol pipettes suggest that the β-blocker is reducing activity of these interneurons and thus the PSA is larger on the timolol pipette than on the saline pipette where no attenuation of the interneuron activity occurs.

2) Second, a high-threshold direct β-receptor action on granule cell membrane supports increased cell firing to a constant input. NE from LC results in an inhibition of a potassium conductance at resting membrane potential most likely through a β-receptor (Lacaille and Swartzkroin, 1988). The main effect of this is an increase in membrane resistance and a small depolarization resulting in an increase in cell-firing to a given synaptic input resulting in the observed increase in PSA of P1 after IDA.

3) Third, dendritic inhibition may be increased by an elevation in NE. Interneurons with axonal arbours restricted to the outer molecular layer (interneuron B), providing feed-forward inhibition to the granule cells may be excited by NE, perhaps through α1-receptors, resulting in a decrease EPSP slope of P1 after IDA. These interneurons are likely to be Molecular Layer Perforant Path-associated (MOPP) cells as described by Han et al., 1993.

74

These neurons. with both axons and dendrites in the molecular layer of the DG are likely to be driven in a feed-forward manner by entorhinal afferents and to influence granule cell dendrites (Freund and Buzsaki. 2000). Alternatively, presynaptic NE heteroreceptors or imidazoline receptors may play a role in this effect.

4) Fourth. NE inhibits somatic feedback disinhibition circuits. NE does not alter early somatic feedback inhibition. LC-NE results in a suppression the effect of feedback disinhibitory interneurons (interneuron C) through an unknown receptor after IDA. This blocks a facilitatory contribution to the local circuit effects at short intervals, resulting in an apparent increase in inhibition after IDA. These interneurons are likely to be IS-1 neurons which stains for calretinin (Freund and Buzsaki. 1996). Their inputs may arise from entorhinal afferents and they innervate mostly neurons terminating on principal cell dendrites (Freund and Buzsaki. 2000). As stimulation currents increase, the facilitation effect is masked or drops out when feed-back inhibitory effects are strongly recruited.

5) Finally. α1-receptor activation enhances firing of feedback dendritic inhibitory interneurons. LC-NE enhances activity of interneuron group D through an α1-receptor, which enhances normal feedback dendritic inhibition on the dentate granule cells resulting in an increase in feedback PPI of EPSP slope after IDA. These interneurons are likely to be Hilar Perforant Path-associated (HIPP) cells as described by Han et al., 1993. HIPP cells are likely to mediate largely feedback inhibition of granules cells by terminating on their dendrites along with entorhinal afferents (Fruend and Buzsaki. 2000).
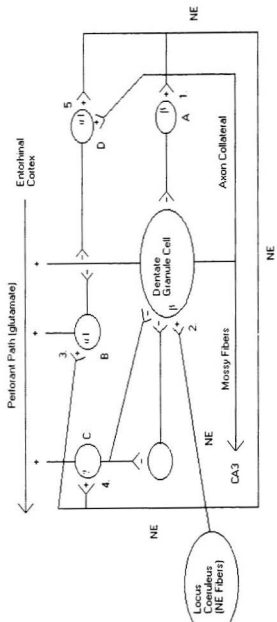
Figure 20

Diagram of proposed model of 5 effects of norepinephrine on local circuit neurons in the dentate gyrus

76

4.6 Conclusions

Like Sara and Bergis (1991) I observed that NE enhances both excitation and inhibition in the DG circuit. However somatic feedback inhibition suggested to be the target of NE action by Sara and Bergis did not appear altered. Rather a reduction of a disinhibitory effect mediated the apparent increase in somatic inhibition seen with short pulses. A novel observation of the present study was that dendritic paired pulse inhibition was enhanced by NE, similar to the change in dendritic inhibition observed with exploration of novel environments. The overall pattern of effects suggests that NE operates by several different mechanisms and produces multiple effects. This is consistent with other studies which have found that NE increases both inhibition and excitation in the cortex (Waterhouse et al, 1980 and 1983; Waterhouse and Woodward, 1980), cerebellum (Woodward et al., 1979) and hippocampus (Segal and Bloom, 1976; Sara and Bergis, 1991). The present study thus adds to the body of evidence that NE is neither an inhibitory nor excitatory neurotransmitter but a neuromodulator that may enhance the signal-to-noise ratio (Segal and Bloom, 1976) and that serves to hone and sharpen the signal thus contributing to selective attention (Sara and Bergis, 1991) and learning/memory. The present study proposes a specific and at least partially testable model of NE local circuit modulation in the DG.

REFERENCES

Amaral. D.G., 1978. A golgi study of cell types in the hilar region of the hippocampus in the rat. J Comp Neurol 182:851-914.

Amaral, D.G. and Witter, M.P. 1989. The three-dimensional organization of the hippocampal formation: a review of anatomic data. Neuroscience 31:571-591.

Andersen, P., Bliss, T.V.P. and Skrede, K.K. 1971. Lamellar organization of hippocampal excitatory pathways. Exp Brain Res 13:222-238.

Andersen, P., Holmquist, B. and Voorhoeve, P.E. 1966. Entorhinal activation of dentate gyrus granule cells. Acta Physiol Scand 66:448-460.

Armstrong, J.N., McIntyre, D.C., Neubort, S. and Sloviter, R.S. 1993. Learning and Memory after adrenalectomy-induced hippocampal dentate granule cell degeneration in the rat. Hippocampus 3(3):359-371.

Assaf, S.Y. Mason, S.T. and Miller, J.J. 1979. Noradrenergic modulation of neuronal transmission between the entorhinal cortex and the dentate gyrus of the rat. J Physiol 292: 52P.

Aston-Jones, G. and Bloom, F.E. 1981a. Activity of Norepinephrine-containing locus coeruleus neurons in behaving rats anticipates fluctuations in the sleep-waking cycle. J Neurosci 1:876-886.

Aston-Jones, G. and Bloom, F.E. 1981b. Norepinephrine-containing locus coeruleus neurons in behaving rats exhibit pronounces responses to non-noxious stimuli. J Neurosci 1:887-900.

Austin, K.B., Bronzino and Morgane, P.J. 1989. Paired_pulse facilitation and inhibition in the dentate is dependent on buhavioural state. Exp Brain Res 77(3):594-604.

Babstock, D.M. and Harley, C.W. 1992. Paragigantocellularis stimulation induces β-adrenergic hippocampal potentiation. Brain Res Bull 28:709-714.

Barnes, C.A. 1988. Spatial Learning and memory processes: the search for their

neurobiological mechanisms in the rat. Trends Neurosci 11:163-169.

Bliss, T.V.P. and Lomo T. 1973. Long-lasting potentiation of synaptic transmission in the dentate area of the anaesthetized rabbit following stimulation of the perforant path. J Physiol 232:3331-3356.

Bliss, T.V., Goddard, G.V. and Riives, M. 1983. Reduction of long-term potentiation in the dentate gyrus of the rat following selective depletion of monoamines. J Physiol 334:475-491.

Bousquet, P., Feldman, J., Tibirica, E., Bricca, G., Greney, H., Dontenwill, M., Stutzmann, J. and Belcourt A. 1992. Imidazoline receptors. A new concept in central regulation of the arterial blood pressure. Am J Hypertens 5(4 Pt 2):47S-50S.

Bramham, C.R., Bacher-Svendsen, K., Sarvey, J.M. 1997. LTP in the lateral perforant path is beta-adrenergic receptor-dependent. Neuroreport 8(3):719-24.

Buckmaster, P.S. and Soltesz, I. 1996. Neurobiology of hippocampal interneurons: A workshop review. Hippocampus 6:330-339.

Butcher S.P., Davis S., Morris R.G. 1990. A dose-related impairment of spatial learning by the NMDA receptor antagonist, 2-amino-5-phosphonovalerate (AP5). Eur Neuropsychopharmacol 1(1):15-20

Buzaki, G. 1984. Feed-forward inhibition in the hippocampal formation. Prog Neurobiol 22:131-153.

Cahill, L., Prins, B., Weber, M. and McGaugh, J.L. 1994. Beta-adrenergic activation and memory for emotional events. Nature 371(6499):702-4.

Carre, G.P. 1993. The effects of glutaminergic activation of the lateral supramammillary nucleus and the medial septum complex on perforant path-evoked potentials, and other physiological parameters, in the dentate gyrus of the rat. Unpublished Doctoral Thesis, Department of Psychology, Memorial University of Newfoundland, St. John's, Newfoundland, Canada.

Cedarbaum, J. and Aghajanian, G. 1978. Activation of locus coeruleus neurons by peripheral stimuli: modulation by a collateral inhibitory mechanism. Life Sci 23:1383-1392.

Chaulk, P and Harley, C.W. 1998. Intracerebroventricular norepinephrine potentiation of the perforant path-evoked potential in the dentate gyrus of anesthetized and awake rats: A role for both α- and β-adrenoreceptor activation. Brain Res 787:59-70.

Clarke, C.G. 1995. Activation of locus coeruleus and concurrent observation of perforant path evoked potential, single unit activity and EEG in the dentate gyrus of the rat. Unpublished Masters Thesis, Department of Psychology, Memorial University of Newfoundland, St. John's, Newfoundland, Canada.

Conrad, C.D. and Roy, E.J. 1993. Selective loss of hippocampal granule cells following adrenalectomy: implications for spatial memory. J Neurosci 13(6):2582-2590.

Dahl, D. and Li, J. 1994. Interactive and discontinuous long-lasting potentiation in the dentate gyrus. NeuroReport 5:1769-1772.

Dahl, D. and Sarvey, J.M. 1989. Norepinephrine induces pathway-specific long-lasting potentiation and depression in the hippocampal dentate gyrus. Proc Natl Acad Sci USA 86:4776-4780.

Dahl, D. and Winson, J. 1985. Action of norepinephrine in the dentate gyrus. I. Stimulation of the locus coeruleus. Exp Brain Res 59:491-496.

Devauges, V. and Sara, S.J. 1990. Activation of the noradrenergic system facilitates and attentional shift in the rat. Behav. Brain Res. 39:19-28.

DiScenna, P.G and Teyler, T.J. 1994. Development of inhibitory and excitatory synaptic transmission in the rat dentate gyrus. Hippocampus 4(5):569-576.

Ennis, M. and Aston-Jones, G. 1986. A potent excitatory input to the nucleus locus coeruleus from the ventrolateral medulla. Neurosci Lett 71:299-305.

Esclapez, M. and Houser, C.R. 1995. Somatostatin neurons are a sub-population of of GABA neurons in the rat dentate gyrus: evidence for co-localization of pre-prosomatostatin and glutamate decarboxylase mRNAs. Neuroscience 64:339-355.

Foote, S.L., Aston-Jones, G. and Bloom F.E. 1980. Impulse activity of locus coeruleus neurons in awake rats and monkeys is a function of sensory stimulation and arousal. Proc Natl Acad Sci USA 77(5):3033-3037.

80

Foote, S.L., Freedman, R. and Oliver, A.P. 1975. Effects of putative neurotransmitters on neuronal activity in the monkey auditory cortex. Brain Res 86:229-242.

Freund, T.F. and Buzsaki, G. Interneurons of the hippocampus. 1996. Hippocampus 6(4):347-470.

Green, E.J., MsNaughton, B.L. and Barnes, C.A. 1990. Exploration-dependent modulation of of evoked responses in fascia dentata: dissociation of motor, EEG and sensory factors and evidence for synaptic efficacy change. J Neurosci 10:1455-1471.

Hagan, J.J., Salamone, J.D., Simpson, J., Iverson, S.F. and Morris, R.G.M. 1988. Place navigation in rats is impaired by lesions of medial septum and diagonal band but not nucleus basalis magnocellularis. Behav Brain Res 27:9-20.

Han, Z.S., Buhl, E.H., Lorinczi, Z. and Somogyi, P. 1993. A high degree of spatial selectivity in the axonal and dendritic domains of physiologically identified local-circuit neurons in the dentate gyrus of the rat hippocampus. Eur J Neurosci 5(5):395-410.

Harley, C.W. 1987. A role for norepinephrine in arousal, emotion and learning?: Limbic modulation by norepinephrine and the Kety hypothesis. Prog. Neuro-Psychopharmacol. and Biol. Psychiat 11:419-458.

Harley, C.W. 1991. Noradrenergic and locus coeruleus modulation of the perforant path-evoked potential in rat dentate gyrus supports a role for the locus coeruleus in attentional and memorial processes. In C.D. Barnes and O. Pompeiano (Eds.) Progress in Brain Research 88, Elsevier Science Publishers, B.V.

Harley, C.W. and Bielajew, C.H. A comparison of glycogen phosphorylase a and cytochrome oxidase histochemical staining in rat brain. 1992. J Comp Neurol 322:377-389.

Harley, C.W and Evans, S. 1988. Locus-coeruleus-induced enhancement of the perforant pat evoked potential: effect of intra-dentate beta-blockers in C.D. Woody, D.L. Alkon & J.L. McGaugh (Eds.), Cellular Mechanisms of conditioning and behavioural plasticity, 415-423. New York: Plenum. pp. 415-423.

Harley, C.W and Milway, J.S. 1986. Glutamate ejection in the locus coeruleus enhances the perforant path-evoked population spike in the denate gyrus. Exp Brain Res 63:143-150.

Harley, C.W., Milway, J.S. and Lacaille, J-C. 1989. Locus coeruleus potentiation of denate gyrus responses: evidence for two systems. Brain Res Bull 22:643-650.

Herreras, O., Solis, J.M., Munoz, M.,Martin del Rio, R. and Lerma, J. 1988. Sensory modulation of hippocampal transmission. I. Opposite effects on CA1 and dentate gyrus synapses. Brain Res 461:290-302.

Hopkins, W.F. and Johnson, D. 1984. Frequency-dependent noradrenergic modulation of long-term potentiation in the hippocampus. Science 226:350-351.

Joy, R.M. and Albertson, T.E. 1993. NMDA receptors have a dominant role in population spike-paired pulse facilitation in the dentate gyrus of urethane-anesthetized rats. Brain Res 604(1-2):273-282.

Kamisaki, Y., Ishikawa, T., Takao, Y., Omidani, H, Kuno, N. and Itoh, T. 1990. Binding of [^{3}H]p-aminoclonidine to two sites, α2-adrenoreceptors and imidazoline binding sites: distribution of imidazoline binding sites in rat brain. Brain Res 514:15-21.

Kety, S.S. The biogenic amines in the central nervous system: 1977. Their possible roles in arrousal, emotion and learning. In F.O. Schmitt (Ed.), The Neurosciences Second Study Program. New York: Rockefeller University Press. pp. 324-335.

Keverne, E.B. and de la Riva, C. 1982. Pheromones in mice: reciprocal interaction between the nose and brain. Nature 296(5853):148-150.

Kitchigina, V., Vankov, A., Harley, C. and Sara, S.J. 1997. Novelty-elicited, noradrenaline-dependent enhancement of excitability in the dentate gyrus. Eur J Neurosci 9:41-47.

Kluver, H. and Bucy, P.C. 1939. Preliminary analysis of functions of the temporal lobe in monkeys. Arch Neurol Psychiat 42:979-1000.

Knight, J.C., Harley, C.W. and Evans, J.H. 1997. Isoproterenol potentiates the perforant path-evoked field potential in dorsal dentate gyrus. Society for Neuroscience Abstracts 23(Pt 2):2041.

Kobayashi, R.M., Palkovits, M., Kopin, I. and Jacobowitz, D.M. 1994. Biochemical mapping of noradrenergic nerves arising from the rat locus coeruleus. Brain Res 77:269-279.

82

Kovacs, G.L., Bohus, B. and Versteeg, D.H.G. 1979. The effects of vasopressin on memory processes: The role of noradrenergic neurotransmission. Neuroscience 4:1529-1537.

Lacaille, J-C. And Harley, C.W. 1985. The action of norepinephrine in the dentate gyrus: beta-mediated facilitation of evoked potentials in vitro. Brain Res 358:210-220.

Lacaille, J-C. And Schwartzkroin, P.A. 1988. Intracellular responses of rat hippocampal granule cells in vitro to discrete applications of norepinephrine. Neurosci Lett 89:176-181.

Leranth, C., Malcom, A.J. and Frotscher, M. 1990. Afferent and efferent synaptic connections of somatostatin-immunoreactive neurons in the rat fascia dentata. J Comp Neurol 295:111-122.

Lomo, T. 1971. Patterns of activation in a monsynaptic cortical pathway: The perforant path input to the dentate area of the hippocampal formation. Exp Brain Res 12:18-45.

Loy, R. Koziell, D.A., Lindsey, J.D. and Moore, R.Y. 1980. Noradrenergic innervation of the adult rat hippocampal formation. J Comp Neurol 189:699-710.

McNaughton, B.L. 1980. Evidence for two physiologically distinct perforant pathways to the fascia dentata. Brain Res 199(1):1-19.

McNaughton, B.L., Barnes, C.A., Meltzer, J. and Sutherland, R.J. 1989. Hippocampal granule cells are necessary for normal spatial learning but not for spatially-selective pyramidal cell discharge. Exp Brain Res 76(3):485-496.

McNaughton, B.L. and Morris, R.G.M. 1987. Hippocampal synaptic enhancement and infromation storage within a distributed memory system. Trends Neurosci 10:408-415.

Mishkin, M. 1978. Memory in monkeys severely impaired by combined but not separate removal of the amygdala and hippocampus. Nature 273:297-298.

Mishkin, M. and Appenzeller, T. 1987. The Anatomy of Memory: An inquiry into the roots of human amnesia has shown how deep structures in the brain may interact with perceptual pathways in outer brain layers to transform sensory stimuli into memories. Sci Am 256:2-11.

Morris, R.G.M., Garrud, P. Rawlings, J. and O'Keefe, L. 1982. Place navigation impaired in rats with hippocampal lesions. Nature 297:681-683.

Morris. R.G.M.. Schlenck. F.. Tweedie. F. and Janard, L.E. 1990. Ibotenate lesions of the hippocampus and/or subiculum: dissociating components of allocentric spatial learning. Eur J Neurosci 2:1016-1028.

Moser, E.I. 1996. Altered inhibition of dentate granule cells during spatial learning in an exploration task. J Neurosci 16(3):1247-1259.

Moser. E. Matheisen, I. and Andersen. P. 1993a. Association between brain temperature abd dentate field potentials in exploring and swimming rats. Science 259:1324-1326.

Moser., E.. Moser M.B. and Andersen, P. 1993b. Synaptic potentiation in the rat dentate gyrus during exploratory learning. NeuroReport 5:317-320.

Moser., E.I.. Moser, M-B. and Andersen. P. 1994. Potentiation of dentate synapses initiated by exploratory learning dissociation from brain temperature, motor activity and arousal. Learn Mem 1:55-73.

Mueller, A.L. Hoffer. B.J. and Dunwiddie, T.V. 1981. Noradrenergic responses in rat hippocampus: evidence for mediation by α and β receptors in the in vitro slice. Brain Res 214:113-126.

Munro. C.A.M.. Walling S.G.. Evans. J.H. and Harley. C.W. 2001. β-adrenergic blockade in the dentate gyrus gyrus in vivo prevents high frequency-induced long-term potentiation of EPSP slope but not long-term potentiation of population spike amplitude. Hippocampus 11:322-328.

Neuman, R. S. and Harley. C.W. 1983. Long-lasting potentiation of the dentate gyrus population spike by norepinephrine. Brain Res 273:162-165.

O'Keefe. J. and Dostrovsky. J. 1971. The hippocampus as a spatial map. Preliminary evidence from unity activity in the freely-moving rat. Brain Res 34(1):171-175.

O'Keefe. J. and Nadel. L. 1971. The Hippocampus as a Cognitive Map. London: Oxford University Press.

Olton, D.S. 1983. Memory functions and the hippocampus. In W. Seifert (Ed.) Neurobiology of the Hippocampus. New York: Freeman. pp. 171-181

Olton, D.S., Becker, J.T. and Handelmann, G.H. 1979. Hippocampus, Space and Memory. Behav Brain Sci 2:313-365.

Olton, D.S. and Papas, B.C. 1979. Spatial memory and hippocampal function. Neuropsychologia 17:669-682.

Pang, K.C. and Rose, G.M. 1987. Differential effects of norepinephrine on hippocampal complex-spike and theta neurons. Brain Res 425(1):146-58.

Paxinos, G. and Watson, C. 1986. The rat brain in stereotaxic coordinates. San Diego: Academic Press Inc.

Pelletier, M.R., Kirkby, R.D., Jones, S.J. and Corcoran, M.E. 1994. Pathway specificity of noradrenergic plasticity in the dentate gyrus. Hippocampus 4(2):181-8.

Pinel, P.J. 1993. BioPsychology - 2nd Edition. Needham Heights, MA: Allyn and Bacon.

Ribak, C.E. Seress, L. and Amaral, D.G. 1985. The development , ultrastructure and synaptic connections of the mossy cells of the dentate gyrus. J Neurocytol 14:835-857.

Richter-Levin, G., Segal, M. and Sara, S.J. 1991. An α2-antagonist enhances EPSP spike coupling in the rat dentate gyrus. Brain Res 540:291-294.

Robinson, G.B., Fluharty S.J., Zigmond M.J., Sclabassi R.J. and Berger T.W. 1993. Recovery of hippocampal dentate granule cell responsiveness to entorhinal cortical input following norepinephrine depletion. Brain Res 614(1-2):21-28.

Robinson, G.B., Racine, R.J. 1985. Long-term potentiation in the dentate gyrus: effects of noradrenaline depletion in the awake rat. Brain Res 325(1-2):71-78.

Rose, G.M. and Pang, K.C. 1989. Differential effect of norepinephrine upon granule cells and interneurons in the dentate gyrus. Brain Res 488(1-2):353-356.

Sara, S.J. and Bergis, O. 1991. Enhancement of excitability and inhibitory processes in hippocampal dentate gyrus by noradrenaline: a pharmacological study in awake free-moving rats. Neurosci Lett 126:1-5.

Sara, S.J. and Devauges, V. 1989. Idazoxan, an α2-antagonist facilitates memory retrieval in

the rat. Behav. Neural Biol 51:401-411.

Sara, S.J., Dyon-Laurent, C. and Herve, A. 1995. Novelty seeking behaviour in the rat dependent upon the integrity of the noradrenergic system. Brain Res Cogn Brain Res 2(3):181-187.

Sara, S.J. and Segal, M. 1991. Plasticity of sensory responses of locus coeruleus neurons in the behaving rat: implications for cognition. Prog Brain Res 88:571-585.

Sara, S.J., Vankov, A. and Herve A. 1994. Locus coeruleus-evoked responses in behaving rats: a clue to the role of noradrenaline in memory. Brain Res Bull 35(5-6):457-65.

Sayin, U., Rutecki, P.A., Mellanby J. and Sutula, T.P. 2001. Gamma-vinyl GABA reduces paired pulse inhibition in the rat dentate gyrus in vivo and in vitro. Epilepsy Res 44(2-3):109-117.

Scharfman, H. Kunkel, D.D. and Schwartzkroin, P.A. 1990. Synaptic connections of dentate granule cells and hilar interneurons: Results of paired intracellular recordings and intracellular horseradish peroxidase injections. Neuroscience 37(3):693-707.

Schlinder, M., Humphrey, P.P.A. and Emson, P.C. 1996. Somatostatin receptors in the central nervous system. Prog Neurobiol 50:9-47.

Scolville, W.B. and Milner, B. 1957. Loss of recent memory after bilateral hippocampal lesions. Journal Neurol Neurosurg and Psychiat 20:11-21.

Segal, M. and Bloom, F.E. The action of norepinephrine in the rat hippocampus. IV. 1976. The effects of locus coeruleus stimulation on evoked hippocampal unit activity. Brain Res 107:513-525.

Sharp, P.E., McNaughton, B.L. and Barnes, C.A. 1989. Exploration-dependent modulation of evoked responses in fascia dentata: fundamental observations and time course. Psychobiol 17:257-269.

Skelton, R.W. and McNamara, R.K. 1992. Bilateral knife cuts to the porforant path disrupt learning in the Morris swim task. Hippocampus 2:73-80.

Sloviter, R.S. 1987. Decreased hippocampal inhibition and a selective loss of interneurons in

experimental epilepsy. Science 235:42-60.

Sloviter. R.S. 1991. Feedforward and Feedback inhibition of hippocampal principal cell activity evoked by perforant path stimulation: GABA-mediated mechanisms that regulate excitability in vivo. Hippocampus 1(1):31-40.

Sloviter. R.S. and Nilaver. G. 1987. Immunocytochemical localization of GABA-cholecystochinin-. vasoactive intestinal polypeptide-. and somatpstatin-like immunoreactivity in the area dentata and hippocampus of the rat. J Comp Neurol 26:42-60.

Squire. L.R. and Zola Morgan. S. 1988. Memory: brain systems and behaviour. Trends Neurosci 11(4):170-175.

Stanton.P.K. and Heinemann, U. 1986. Norepinephrine enhances stimulus-evoked calcium and potassium concentration changes in dentate granule cell layer. Neurosci Lett 67(3):233-8.

Stanton. P.K. Mody. I and Heinemann. U. 1989. A role for N-methyl-D-aspartate in norepinephrine-induce long-lasting potentiation in the dentate gyrus. Exp Brain Res 77(3):517-530.

Stanton. P.K. and Sarvey. J.M. 1985a. Depletion of norepinephrine, but not serotonin. reduces long-term potentiation in the dentate gyrus of rat hippocampal slices. J Neurosci 5(8):2169-2176.

Stanton. P.K.. Sarvey. J.M. 1985b. Blockade of norepinephrine-induced long-lasting potentiation in the hippocampal dentate gyrus by an inhibitor of protein synthesis. Brain Res 361(1-2):276-283.

Stanton. P.K. and Sarvey, J.M. 1987. Norepinephrine regulates long-term potentiation of both the population and dendritic EPSP in hippocampal dentate gyrus. Brain Res Bull 18:115-119.

Steward. O.. Tamasulo, R. and Levy, W.B. 1990. Blockade of inhibition in a pathway with dual excitatory and inhibitory action unmasks a capability for LTP that is otherwise not expressed. Brain Res 516:292-300.

Sutherland. R.J.. Kolb. B. and Wishaw. I.Q. 1982. Spatial mapping: definitive disruption by

hippocampal or medial frontal cortical damage in the rat. Neurosci Lett 31:271-276.

Sutherland, R.J., Wishaw, I.Q. and Kolb, B. 1983. A behavioural analysis of spatial localization following electrolytic, kainate- or colchicine-induced damage to the hippocampal formation in the rat. Behav Brain Res 7:133-153.

Teyler, T.J. and Discena, P. 1984. Long-term potentiation as a candidate mnemonic device. Brain Res Rev 7:15-28.

Thomas, D.N. and Holman, R.B. 1998. A microdialysis study of the regulation of endogenous noradrenalin release in the rat hippocampus.. J. Neurochem., 56 (1991) 1741-1746.

Ugedo, L., Pineda, J., Ruiz-Ortega, J.A and Martin-Ruiz, R. Stimulation of locus coeruleus neurons by non-I_1/I_2-type imidazoline receptors: an in vivo and in vitro electrophysiological study. Br J Pharmacol 125(8):1685-94.

Unerstall, J.R., Kopajtic, T.A. and Kuhar, M.J. 1984. Distribution of $\alpha2$-agonist binding sites in the rat and human central nervous system: Analysis of some functional, anatomic correlates of the pharmacologic effects of clonidine and related adrenergic agents. Brain Res Rev 7:69-101.

Vankov, A., Herve-Minvielle, A.and Sara, S.J. 1995. Response to novelty and its rapid habituation in locus coeruleus neurons of the freely exploring rat. Eur J Neurosci 7(6):1180-1187.

Walsh, T.J., Schulz, D.W., Tilson, H.A. and Schmechel, D.E. 1986. Colchicine-induced granule cell loss in rat hippocampus: selective behavioural and histological alternations. Brain Res 398(1):23-26.

Washburn, M. and Moises, H.C. 1989. Electrophysiological correlates of presynaptic alpha 2-receptor-mediated inhibition of norepinephrine releaase at locus coeruleus synapses in dentate gyrus. J of Neurosci 9:2131-2140.

Watebe, K. and Satoh, T. 1980. Cross-correlation analysis of neuronal activities in bilateral nuclei of locus coeruleus. Brain Res 199(1):231-234.

Waterhouse, B.D., Moises, H.C. and Woodward, D.J. 1980. Noradrenergic modulation of sematosemsory cortical neuronal responses to iontophoretically-applied putative

neurotransmitters. Exp Neurol 69:30-69.

Waterhouse, B.D., Azizi, S.A., Burne, R.A and Woodward, D.J. 1983. Interactions of norepinephrine and serotonin with vissually-evoked responses of simple and complex cells in area 17 of rat cortex. Society for Neuroscience Abstracts 9:1001.

Waterhouse, B.D. and Woodward, D.J. 1980. Interaction of norepinephrine with cerebrocortical activity evoked by stimulation of sematosensory afferent pathways in the rat. Exp Neurol 67:11-34.

Winson, J.and Abzug, C. 1978. Neuronal transmission through hippocampal pathways dependent on behaviour. J Neurophysiol 41:716-732.

Winson, J. and Dahl, D. 1985. Action of norepinephrine in the dentate gyrus. II. Iontophoretic studies. Exp Brain Res 59:497-506.

Woodward, D.J., Moises, H.C., Waterhouse, B.D., Hoffer, B.J. and Freedman, R. 1979. Modulatory actions of norepinephrine in the central nervous system. Fed Proc 38:2109-2116.

Zola-Morgan, S. Squire, L.R. and Mishkin, M. 1982. Neuroanatomy of amnesia: amygdala-hippocampus versus temporal stem. Science 218:1337-1339.

Zola-Morgan, S. and Squire, L.R. 1985. Medial temporal lesions in monkeys impair memory in a variety of tasks sensitive to human amnesia. Behav Neurosci 100:165-170.